

SPACE RADIATION SHIELDING WITH THE MAGNETIC FIELD OF A CYLINDRICAL SOLENOID

by P. F. McDonald
T. J. Buntyn

GPO PRICE \$ _____

CFSTI PRICE(S) \$ _____

Hard copy (HC) 3.00

Microfiche (MF) FL

REF ID: A66396

June 1966

N66 39691

FACILITY FORM 602

(ACCESSION NUMBER)

(PAGES)

(NASA CR OR TMX OR AD NUMBER)

(THRU)

(CODE)

(CATEGORY)

RESEARCH LABORATORIES

BROWN ENGINEERING COMPANY, INC.

HUNTSVILLE, ALABAMA

TECHNICAL NOTE R-203

SPACE RADIATION SHIELDING WITH THE
MAGNETIC FIELD OF A CYLINDRICAL SOLENOID

June 1966

Prepared For

NUCLEAR AND PLASMA PHYSICS BRANCH
RESEARCH PROJECTS LABORATORY
GEORGE C. MARSHALL SPACE FLIGHT CENTER

Prepared By

RESEARCH LABORATORIES
BROWN ENGINEERING COMPANY, INC.

Contract No. NAS8-20166

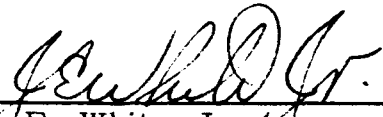
Prepared By

P. F. McDonald
T. J. Buntyn

ABSTRACT

The charged-particle radiation shielding characteristics of magnetic fields generated by right circular solenoids are analyzed using Störmer's theory. Allowed and forbidden regions for unbound particle motion are obtained and shielded volumes are presented in parametric form. The results are applicable over a wide range of particle energies and solenoid parameters through the Störmer transformation.

Approved:



J. E. White, Jr.
Research Projects Coordinator

Approved:



R. C. Watson, Jr.
Vice President
Advanced Systems & Technologies

TABLE OF CONTENTS

	Page
INTRODUCTION	1
STÖRMER'S THEOREM	3
VECTOR POTENTIAL	5
ALLOWED AND FORBIDDEN REGIONS OF UNTRAPPED PARTICLE MOTION	9
SHIELDING EFFECTIVENESS	27
CONCLUSIONS	33
REFERENCES	35
APPENDIX A - COEFFICIENTS FOR EXPANSION OF THE VECTOR POTENTIAL	37
APPENDIX B - COMPUTER PROGRAM	39

LIST OF FIGURES

Figure		Page
1	Reference Coordinate System	4
2	Cylindrical Solenoid	6
3	The Störmer Unit of Length as a Function of Magnetic Moment	10
4	Allowed and Forbidden Regions of Charged Particle Motion About a Solenoid for $\bar{\gamma} < \bar{\gamma}_c$ ($\bar{\gamma} = -1.0$, $\lambda = 0.169$, $\eta/\lambda = 2$)	12
5	Allowed and Forbidden Regions of Charged Particle Motion About a Solenoid for $\bar{\gamma} = \bar{\gamma}_c$ ($\bar{\gamma} = -0.97533$, $\lambda = 0.169$, $\eta/\lambda = 2$)	13
6	Allowed and Forbidden Regions of Charged Particle Motion About a Solenoid for $\bar{\gamma} > \bar{\gamma}_c$ ($\bar{\gamma} = -0.95$, $\lambda = 0.169$, $\eta/\lambda = 2$)	14
7	Allowed and Forbidden Regions of Charged Particle Motion About a Solenoid for $\bar{\gamma} = \bar{\gamma}_c$ ($\bar{\gamma} = -1.0004$, $\lambda = 0.048$, $\eta/\lambda = 0.25$)	17
8	Allowed and Forbidden Regions of Charged Particle Motion About a Solenoid for $\bar{\gamma} = \bar{\gamma}_c$ ($\bar{\gamma} = -0.998$, $\lambda = 0.048$, $\eta/\lambda = 2$)	18
9	Allowed and Forbidden Regions of Charged Particle Motion About a Solenoid for $\bar{\gamma} = \bar{\gamma}_c$ ($\bar{\gamma} = -1.0013$, $\lambda = 0.086$, $\eta/\lambda = 0.25$)	19
10	Allowed and Forbidden Regions of Unbound Charged Particle Motion About a Solenoid for $\bar{\gamma} = \bar{\gamma}_c$ ($\bar{\gamma} = -0.9995$, $\lambda = 0.086$, $\eta/\lambda = 1$)	20
11	Allowed and Forbidden Regions of Unbound Charged Particle Motion About a Solenoid for $\bar{\gamma} = \bar{\gamma}_c$ ($\bar{\gamma} = -0.994$, $\lambda = 0.086$, $\eta/\lambda = 2$)	21

LIST OF FIGURES (Continued)

Figure		Page
12	Allowed and Forbidden Regions of Unbound Charged Particle Motion in the Field of a Solenoid for $\bar{\gamma} = \bar{\gamma}_c$ ($\bar{\gamma} = -1.005$, $\lambda = 0.169$, $\eta/\lambda = 0.25$)	
13	Allowed and Forbidden Regions of Unbound Charged Particle Motion in the Field of a Solenoid for $\bar{\gamma} = \bar{\gamma}_c$ ($\bar{\gamma} = -0.998$, $\lambda = 0.169$, $\eta/\lambda = 1$)	23
14	Allowed and Forbidden Regions of Unbound Charged Particle Motion in the Field of a Solenoid for $\bar{\gamma} = \bar{\gamma}_c$ ($\bar{\gamma} = -1.030$, $\lambda = 0.427$, $\eta/\lambda = 0.25$)	
15	Allowed and Forbidden Regions of Unbound Charged Particle Motion in the Field of a Solenoid for $\bar{\gamma} = \bar{\gamma}_c$ ($\bar{\gamma} = -0.983$, $\lambda = 0.427$, $\eta/\lambda = 1$)	25
16	Shielding Effectiveness in the Partially Shielded Region of a Solenoid ($\lambda = 0.314$, $\eta/\lambda = 0.25$)	30
17	Totally Shielded and Partially Shielded Volumes for the Right Circular Solenoid as a Function of Coil Radius	31

LIST OF SYMBOLS

\vec{A}	Magnetic vector potential
A_ϕ	ϕ component of the vector potential
C_{in}	Central field expansion coefficients
C_{on}	Remote field expansion coefficients
C_{st}	Störmer unit of length
dl	Width of differential current element
E	Particle energy
$\mathcal{G}(\vec{r}, E)$	Shielding effectiveness at \vec{r} for particles with energy E
I	Current
j	Current density per unit length
L	Length of solenoid
M	Magnetic moment of the solenoid
n	Summation index
p	Magnitude of particle momentum
Q	See Equation 1
R	Radius of solenoid
(r, θ, ϕ)	Spherical polar coordinates
(r', ψ, ϕ)	Spherical coordinates of source point on the solenoid
\vec{v}	Particle velocity
v	$= \vec{v} $
v_ϕ	ϕ component of velocity

LIST OF SYMBOLS (Continued)

α	$\equiv \pi/2$ if $r < R$
	$\equiv \beta$ if $r > R/\sin \beta$
	$\equiv \sin^{-1} (R/r)$ if $R < r < R/\sin \beta$
β	$\equiv \tan^{-1} \frac{2R}{L}$
γ	Impact parameter
$\bar{\gamma}$	Dimensionless impact parameter
δ	See Figure 1
η	$L/2 C_{st}$
μ	Permeability (mks units)
ρ	r/C_{st}
ω	Angle between \vec{v} and $-\hat{\phi}$

INTRODUCTION

Magnetic shielding of spacecraft against charged-particle radiation has been considered by several authors (see References 1 through 10 and the Bibliography¹¹). The advantages of active shielding over passive shielding have been discussed by these investigators. The principal advantages are radiation shielding system weight reduction and prevention of the generation of secondary radiation by high energy particles. Weight savings compared to passive shielding systems are possible when superconducting magnets are used to generate the very high magnetic fields required. Although the magnets are not presently available, rapid advances in superconducting magnet technology indicate that it will soon be possible to produce the necessary high fields with very modest power consumption. The second advantage is possible when an unconfined magnetic field diverts the primary particle away from the space vehicle instead of allowing it to enter material where it may generate a large shower of secondary particles which may cause more radiation damage than would the primary particle if no shielding at all were used.

The shielding characteristics of the dipole and current loop magnetic fields have been analyzed in sufficient detail in References 2 through 10 and 12 through 14. Tooper⁸ presented the vector potential of a finite cylindrical solenoid and one example of the allowed and forbidden regions for this type field. It was felt that the shielding characteristics of the finite right circular solenoid are of sufficient importance to justify further analysis. This paper extends the analysis of the shielding geometry and shielding effectiveness for the cylindrical solenoid for a range of solenoid parameters and particle energies. The analysis and calculated results should be useful to those concerned with the design of magnetic shielding systems for spacecraft.

STÖRMER'S THEOREM

Störmer¹² obtained a first integral to the equations of motion for a charged particle in an axisymmetric magnetic field. Discussions of this integral are found in many places, e. g., O'Rear¹⁴. This integral is known as Störmer's theorem and may be written in the form (Urban¹⁵, Stern¹⁶)

$$Q = \cos \omega = -\frac{v_\phi}{v} = \frac{2\gamma}{r \sin \theta} + \frac{q A_\phi}{p} \quad (1)$$

where (r, θ, ϕ) are the spherical coordinates; γ is the impact parameter or the perpendicular distance from the axis of the field source to the trajectory which the particle would follow if the field were not present; q is the charge of the particle (coulombs); ω is the angle between $-\hat{\phi}$ and the velocity vector, v_ϕ is the ϕ component of velocity, p and v are the magnitudes of particle momentum and velocity and A_ϕ is the magnitude of the vector potential,

$$\vec{A} = A_\phi \hat{\phi} \quad (2)$$

Figure 1 shows the coordinates used in describing the particle motion.

Since Q given in Equation 1 is the cosine of an angle, $|Q|$ can only take on values less than or equal to unity for real particle motion. As r , θ , γ and p are allowed to vary over all reasonable values, Q takes on values such that $|Q| > 1$. Regions of phase space where $|Q| > 1$ are forbidden to unbound particles.

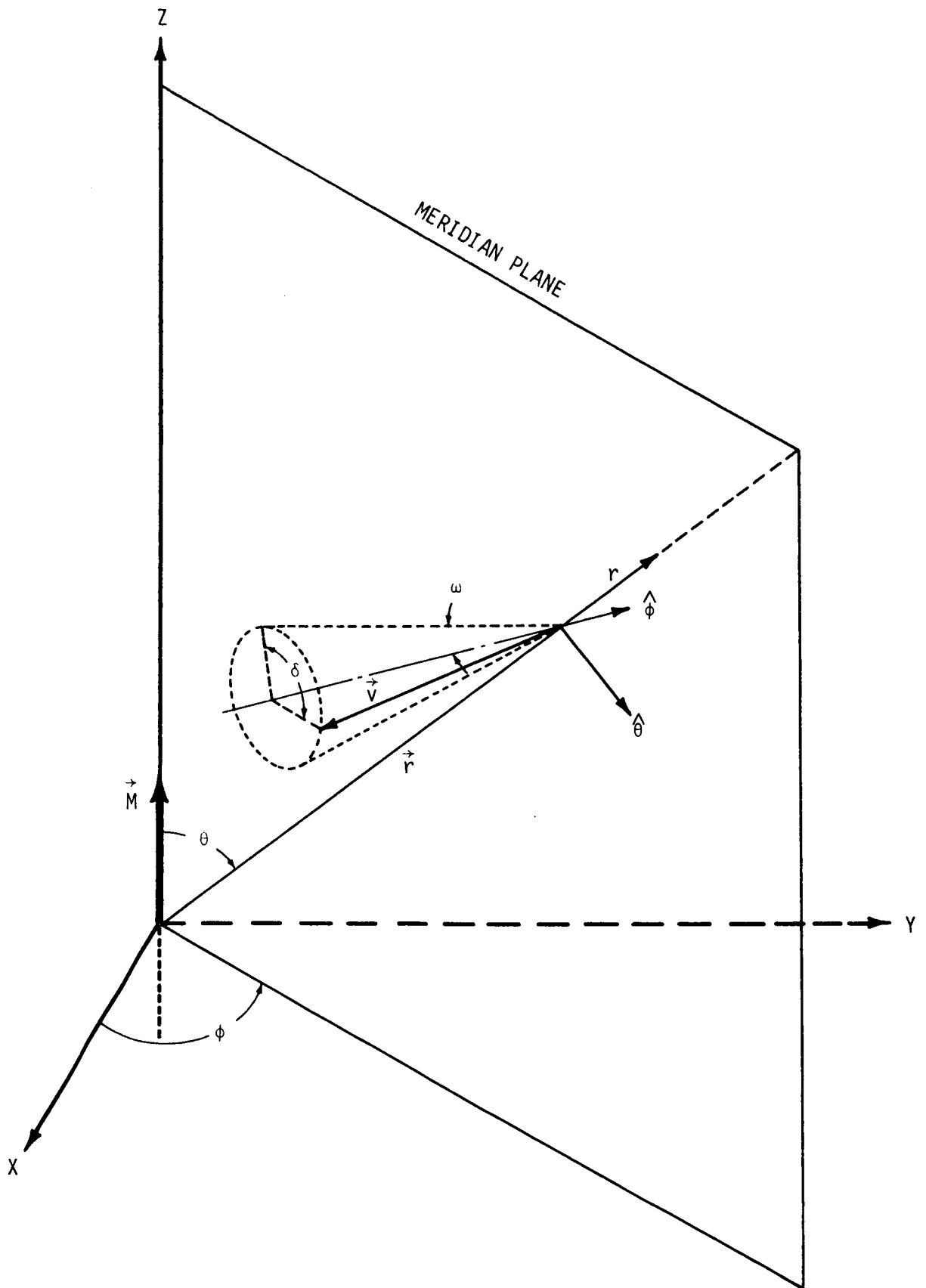


Figure 1. Reference Coordinate System

VECTOR POTENTIAL

The vector potential of the finite solenoid may be found by considering the solenoid to be composed of a large number of thin circular strips of width $d\ell$, each carrying a current dI . The vector potential of one of these strips at $r = r'$, $\theta = \psi$ is given in terms of the associated Legendre polynomials by (Smythe¹⁹)

$$dA_{\phi} = \frac{\mu_0 dI}{2} \sum_{n=1}^{\infty} \frac{\sin \psi}{n(n+1)} \left(\frac{r'}{r}\right)^n P_n^1(\cos \psi) P_n^1(\cos \theta) \quad (3a)$$

if $r < r'$, or by

$$dA_{\phi} = \frac{\mu_0 dI}{2} \sum_{n=1}^{\infty} \frac{\sin \psi}{n(n+1)} \left(\frac{r'}{r}\right)^{n+1} P_n^1(\cos \psi) P_n^1(\cos \theta) \quad (3b)$$

if $r > r'$. μ_0 is the permeability of free space and the geometry is depicted in Figure 2.

The vector potential of the solenoid is obtained by summing the contribution of the infinitesimal loops or

$$A_{\phi} = \int dA_{\phi} \quad (4)$$

From Figure 2 it is evident that

$$\sin \psi = \frac{R}{r'} = r' \frac{d\psi}{d\ell}, \quad r' = \frac{R}{\sin \psi} \quad \text{and} \quad d\ell = \frac{R d\psi}{\sin^2 \psi} \quad (5)$$

The infinitesimal current dI is equal to $j d\ell$ where j is the current density per unit length along the solenoid which is assumed to be constant. Now the integration may be performed over the angle ψ . The vector potential for the region $r < R$ is given by

$$A_{\phi} = \frac{\mu_0 j R}{2} \sum_{n=1}^{\infty} \frac{C_{in}(\beta)}{n(n+1)} \left(\frac{r}{R}\right)^n P_n^1(\cos \theta) \quad (6)$$

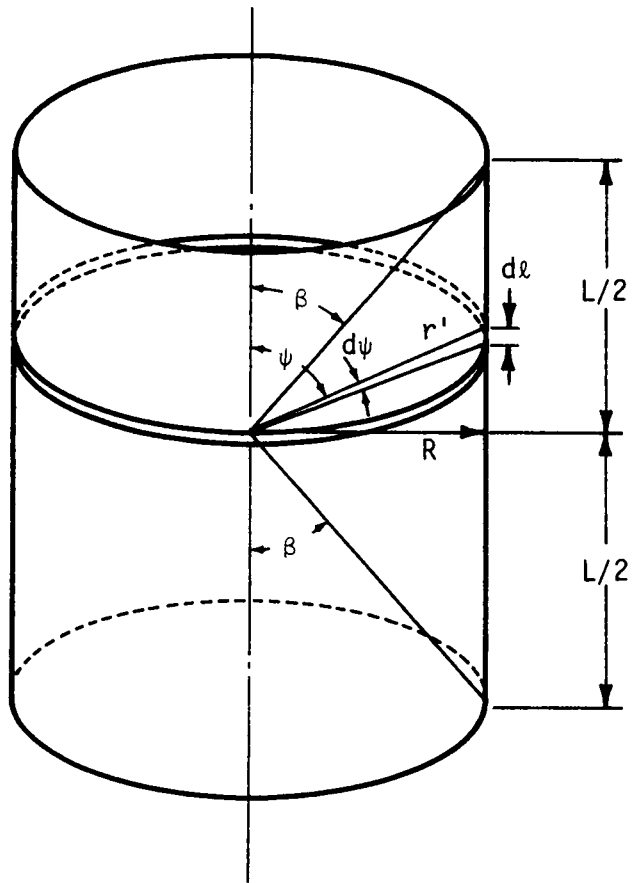


Figure 2. Cylindrical Solenoid

where

$$C_{in}(\beta) = \int_{\beta}^{\pi-\beta} (\sin \psi)^{n-1} P_n^1(\cos \psi) d\psi \quad , \quad (7)$$

and for the region $r > R/\sin \beta$, it is

$$A_{\phi} = \frac{\mu_0 j R}{2} \sum_{n=1}^{\infty} \frac{C_{on}(\beta)}{n(n+1)} \left(\frac{R}{r}\right)^{n+1} P_n^1(\cos \theta) \quad (8)$$

where

$$C_{on}(\beta) = \int_{\beta}^{\pi-\beta} \frac{P_n^1(\cos \psi) d\psi}{(\sin \psi)^{n+2}} \quad (9)$$

and

$$\beta = \tan^{-1} \frac{2R}{L} \quad .$$

In the intermediate region where $R < r < R/\sin \beta$, the vector potential is given by

$$A_{\phi} = \frac{\mu_0 j R}{2} \sum_{n=1}^{\infty} \frac{P_n^1(\cos \theta)}{n(n+1)} \left\{ [C_{in}(\beta) - C_{in}(\alpha)] \left(\frac{r}{R}\right)^n + C_{on}(\alpha) \left(\frac{R}{r}\right)^{n+1} \right\} \quad (10)$$

where

$$\alpha \equiv \sin^{-1} \left(\frac{R}{r}\right) \quad .$$

Equation 10 may be used also in the regions $r < R$ and $r > R/\sin \beta$ if α is redefined in these intervals to be $\alpha \equiv \frac{\pi}{2}$ if $r < R$, or $\alpha \equiv \beta$ if $r > R/\sin \beta$.

Since the current distributions considered are symmetric with respect to the xy plane, the coefficients of the $P_n^1(\cos \theta)$ terms for n even must be zero.

Expressions for C_{in} and C_{on} were derived out to $n = 11$ and are given in Appendix A. The infinite series were terminated after the $P_{11}^1(\cos \theta)$ term in all the calculations. The result of the termination of the series is similar to that found by giving the current sheet a finite thickness instead of zero thickness. Tooper⁸ finds a singular point in the vector potential at the edge of solenoid using the thin sheet assumption for the current distribution. The singularity does not appear in this approximation to the vector potential.

The magnetic moment of the solenoid is given by

$$M = \pi R^2 j L \quad . \quad (11)$$

ALLOWED AND FORBIDDEN REGIONS OF UNTRAPPED PARTICLE MOTION

The insertion of Equations 10 and 11 into Equation 1 yields Störmer's theorem for a solenoid,

$$Q = \frac{2\bar{\gamma}}{r \sin \theta} + \frac{q \mu_0 M}{2 \pi p R L} \sum_{n=1}^{\infty} \frac{P_n^1(\cos \theta)}{n(n+1)} \left\{ [C_{in}(\beta) - C_{in}(\alpha)] \left(\frac{r}{R}\right)^n + C_{on}(\alpha) \left(\frac{R}{r}\right)^{n+1} \right\} \quad (12)$$

Equation 12 may be made dimensionless by defining the Störmer unit of length

$$C_{st}^2 = \frac{q \mu_0 M}{4 \pi p} \quad (13)$$

and the dimensionless quantities,

$$\lambda \equiv R/C_{st}, \quad \rho \equiv r/C_{st}, \quad \bar{\gamma} \equiv \gamma/C_{st} \quad \text{and} \quad \eta \equiv L/2 C_{st} \quad (14)$$

Figure 3 shows C_{st} versus $\mu_0 M$ for selected particle energies. Substituting Equations 13 and 14 into Equation 12 yields the dimensionless Störmer theorem for a solenoid,

$$Q = \frac{2\bar{\gamma}}{\rho \sin \theta} + \frac{1}{\lambda \eta} \sum_{n=1}^{\infty} \frac{P_n^1(\cos \theta)}{n(n+1)} \left\{ [C_{in}(\beta) - C_{in}(\alpha)] \left(\frac{\rho}{\lambda}\right)^n + C_{on}(\alpha) \left(\frac{\lambda}{\rho}\right)^{n+1} \right\} \quad (15)$$

Tooper⁸ has given Q for a cylindrical solenoid in terms of the complete and incomplete elliptic integrals. Störmer's theory for dipole fields, multipole fields and ring current fields has been discussed extensively in the literature (see, for example, References 4-6, 9, 12-18). Equation 15 permits the determination of allowed and forbidden regions of unbound charged particle motion.

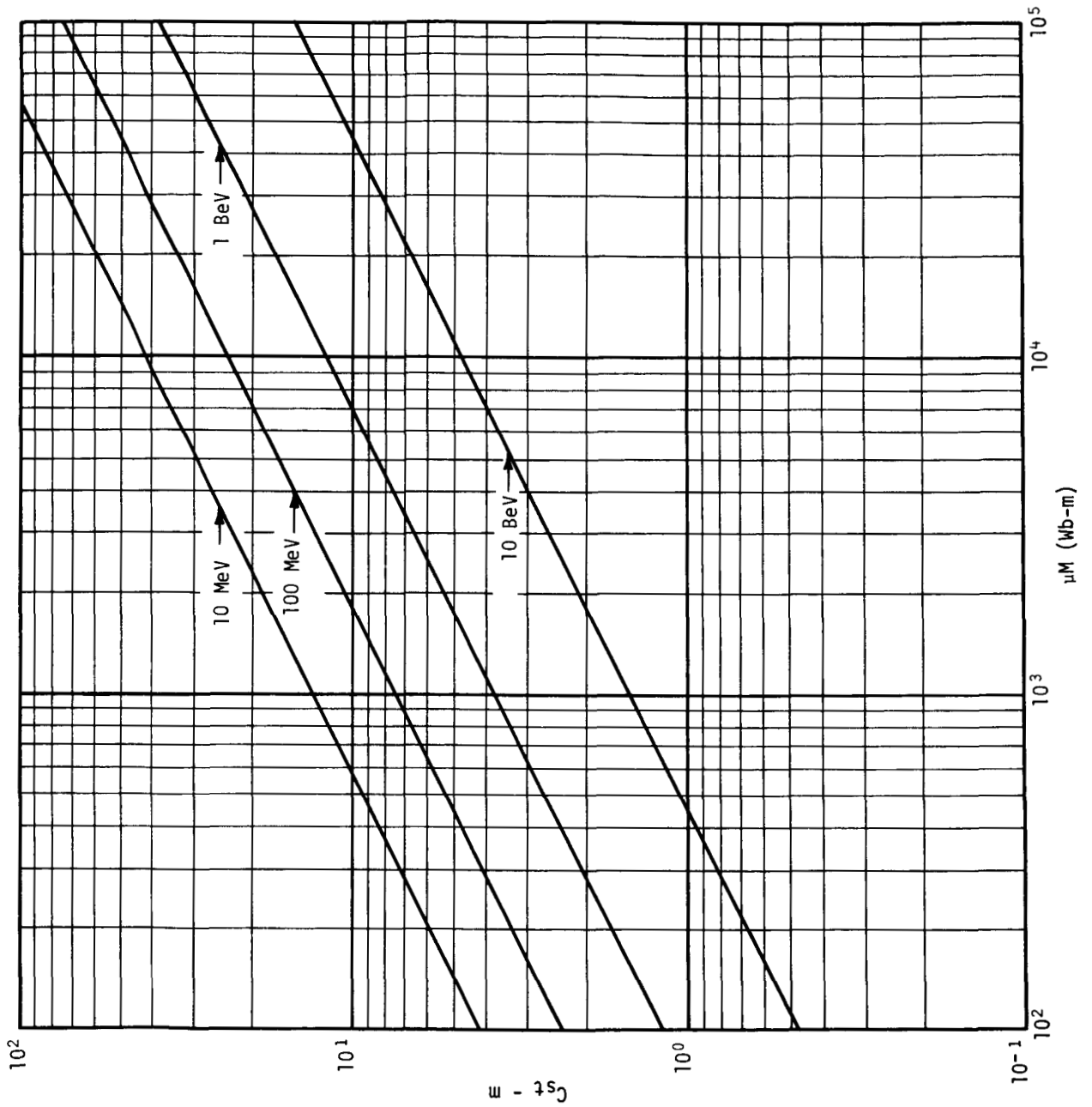


Figure 3. The Störmer Unit of Length as a Function of Magnetic Moment and Proton Kinetic Energy

For given particle energy and solenoid parameters, the shapes of the allowed and forbidden regions are strongly dependent on the impact parameter $\bar{\gamma}$. Figures 4, 5 and 6 illustrate the variation of the allowed and forbidden regions in "Störmer space" with increasing $\bar{\gamma}$. The forbidden regions are shaded and the allowed regions are unshaded in these figures. In Figure 4 there is a forbidden region at the solenoid where $Q > 1$ which is surrounded by an allowed region with $-1 < Q < 1$. These will be referred to as the inner forbidden and allowed regions, respectively. Surrounding these regions is an outer forbidden region where $Q < -1$ and finally there is an outer allowed region near $\theta = \pi/2$ where $-1 < Q < 0$. In Figure 5 it is found that the inner allowed and the outer allowed regions just come together at a pass point for a certain value of $\bar{\gamma}$. The $\bar{\gamma}$ value for this condition is called the critical impact parameter, $\bar{\gamma}_c$. It is seen in Figure 6 that further increase of the impact parameter opens the pass connecting the inner allowed and outer allowed regions and particles may enter the inner allowed region from infinity. The Q surface for $\bar{\gamma} = \bar{\gamma}_c$ provides the information needed to study the shielding properties of the field. The forbidden region for which $Q_c > 1$ which surrounds the equatorial part of the solenoid shell is the completely shielded region for particles of a specific energy. Surrounding this region is the inner allowed region where $-1 < Q < 1$. This region is allowed for some particle directions and forbidden to other directions and is, therefore, the partially shielded region. The outer forbidden region ($Q < -1$) and the outer allowed region ($-1 < Q < 0$) are both completely unshielded for particles from infinity.

It has been found (Urban^{15, 18}, Prescott¹³, Prescott, et al.¹⁷) that the existence of a pass point in the projection of the Q surface on the (ρ, θ) plane at $\bar{\gamma} = \bar{\gamma}_c$ coincides with the existence of a saddle point in the Q surface. It is also to be noted that for this type field the saddle point of interest occurs at the $Q = -1$ contour of the $Q(\bar{\gamma}_c)$ surface. These two conditions facilitate the location of the pass points and the determination of the critical impact parameter for which the pass point just closes.

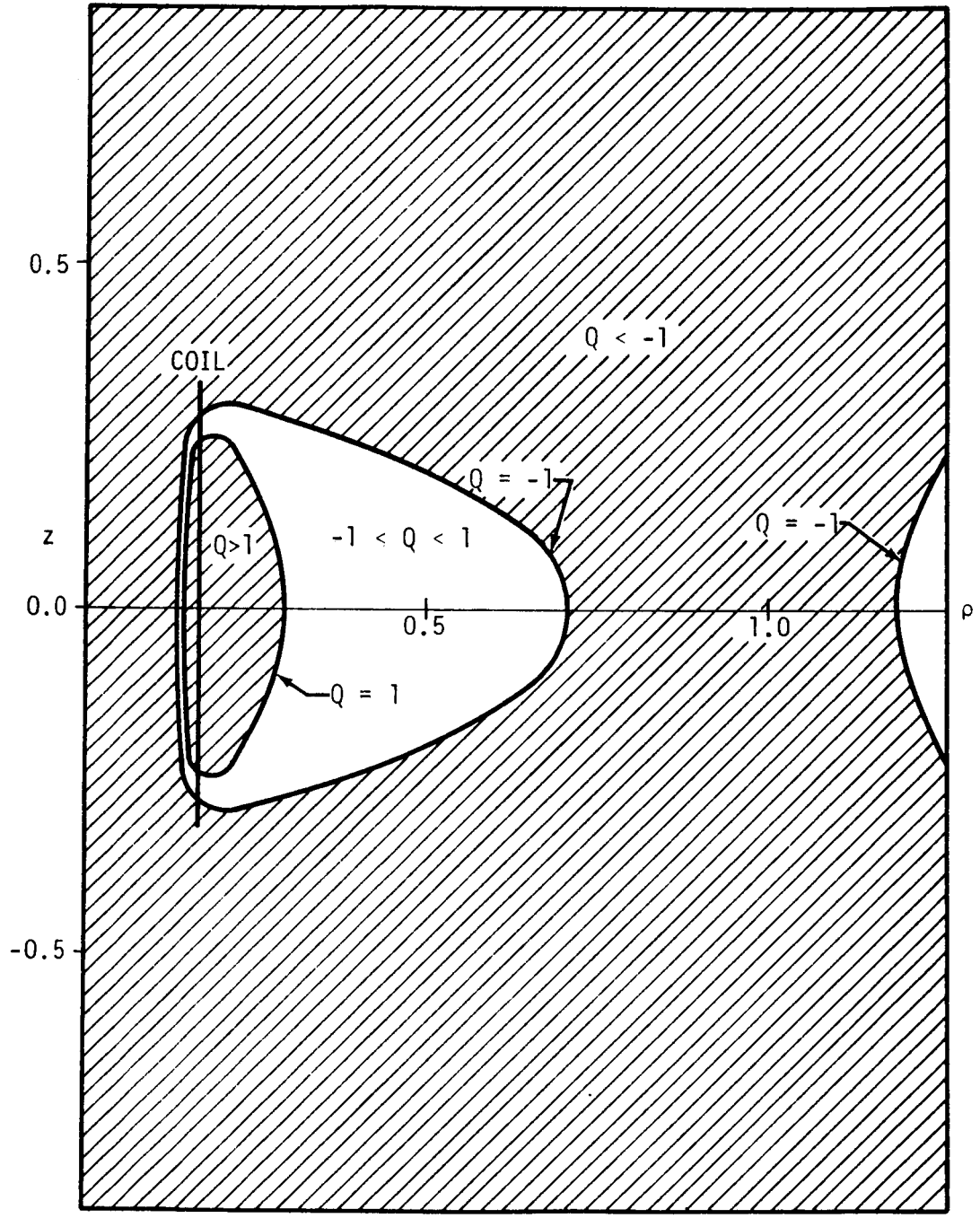


Figure 4. Allowed and Forbidden Regions of Charged Particle Motion About a Solenoid for $\bar{\gamma} < \bar{\gamma}_c$ ($\bar{\gamma} = -1.0$, $\lambda = 0.169$, $\eta/\lambda = 2$)

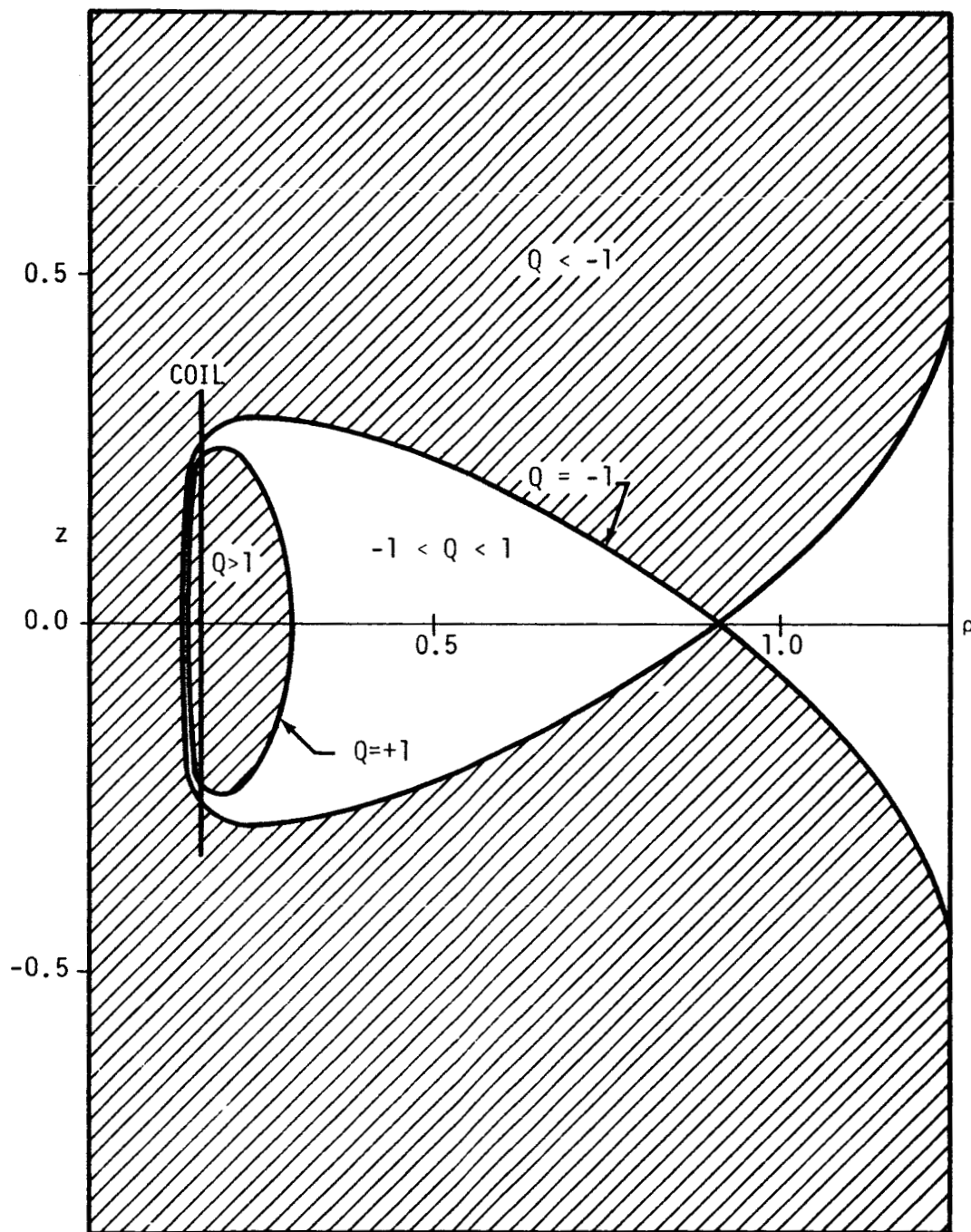


Figure 5. Allowed and Forbidden Regions of Charged Particle Motion About a Solenoid for $\bar{\gamma} = \bar{\gamma}_c$ ($\bar{\gamma} = -0.97533$, $\lambda = 0.169$, $n/\lambda = 2$)

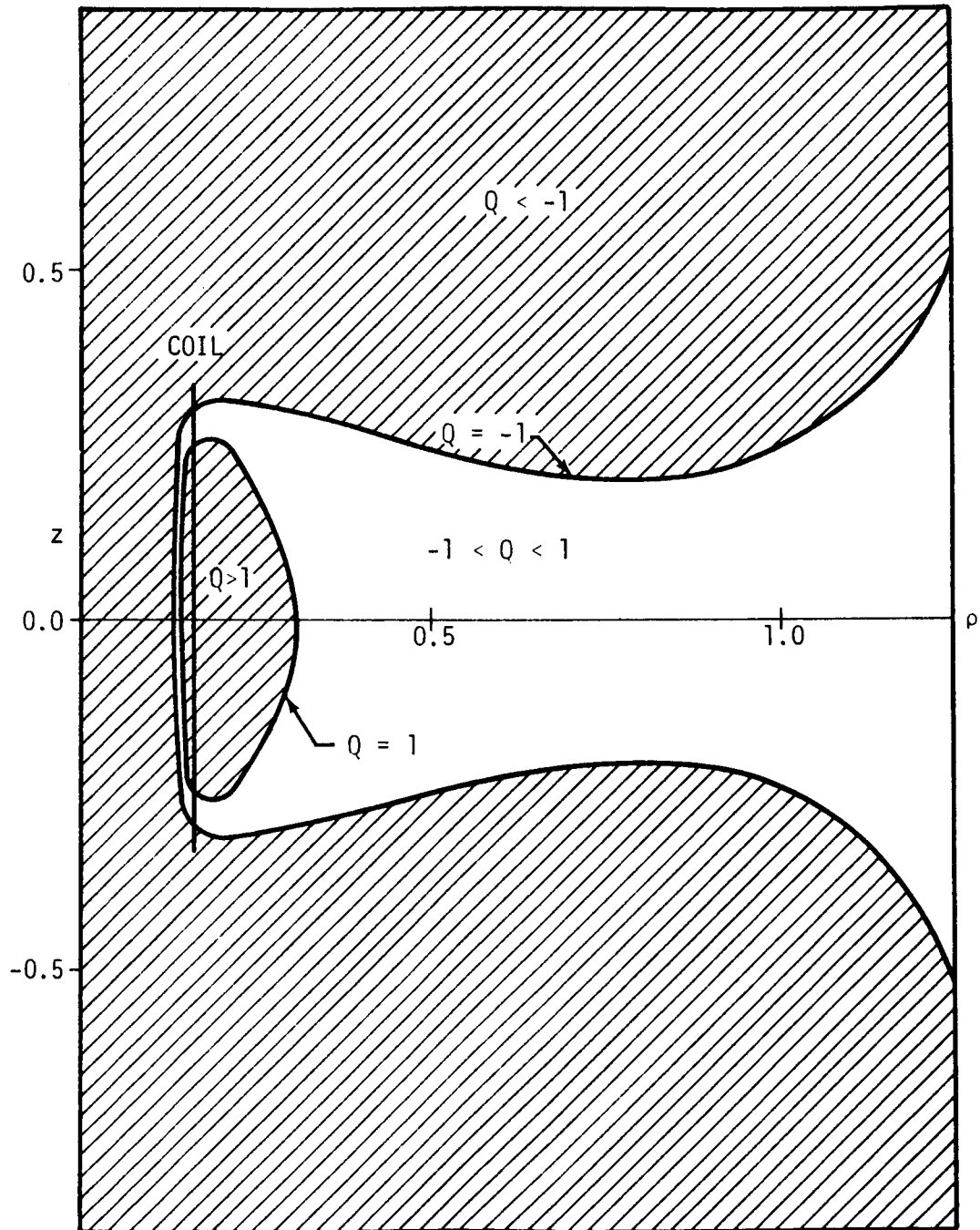


Figure 6. Allowed and Forbidden Regions of Charged Particle Motion About a Solenoid for $\bar{\gamma} > \bar{\gamma}_c$ ($\bar{\gamma} = -0.95$, $\lambda = 0.169$, $\eta/\lambda = 2$)

The necessary and sufficient conditions which must be satisfied for a function $F(\rho, \theta)$ at a given point in order that the point be a saddle point in the function are

$$\left. \frac{\partial F}{\partial \rho} \right|_{(\rho_c, \theta_c)} = 0, \quad \left. \frac{1}{\rho} \frac{\partial F}{\partial \theta} \right|_{(\rho_c, \theta_c)} = 0 \quad (16)$$

and

$$\left[\left(\frac{1}{\rho} \frac{\partial^2 F}{\partial \rho \partial \theta} \right)^2 \right]_{(\rho_c, \theta_c)} - \left[\left(\frac{\partial^2 F}{\partial \rho^2} \right) \left(\frac{1}{\rho^2} \frac{\partial^2 F}{\partial \theta^2} \right) \right]_{(\rho_c, \theta_c)} > 0 \quad (17)$$

When Equations 16 are applied to Equation 15

$$\begin{aligned} \frac{\partial Q_c}{\partial \rho} = & - \frac{2 \bar{Y}_c}{\rho_c^2 \sin \theta} + \frac{1}{\lambda \eta} \sum_{n=1}^{\infty} P_n^1(\cos \theta) \left\{ \frac{[C_{in}(\beta) - C_{in}(\alpha)]}{n+1} \frac{\rho_c^{n-1}}{\lambda^n} \right. \\ & \left. - \frac{C_{on}}{n} \frac{\lambda^{n+1}}{\rho_c^{n+2}} + \frac{2 P_n^1(\cos \alpha)}{n(n+1) \cos \alpha} \left[-\rho_c^n \left(\frac{\sin \alpha}{\lambda} \right)^{n+1} + \frac{1}{\rho_c^{n+1}} \left(\frac{\lambda}{\sin \alpha} \right)^n \right] \right\} = 0 \end{aligned} \quad (18)$$

and

$$\begin{aligned} \frac{1}{\rho} \frac{\partial Q_c}{\partial \theta} = & - \frac{2 \bar{Y}_c \cos \theta}{\rho_c^2 \sin^2 \theta} + \frac{1}{\rho_c \lambda \eta} \sum_{n=1}^{\infty} \frac{1}{n(n+1)} \left\{ [C_{in}(\beta) - C_{in}(\alpha)] \left(\frac{\rho_c}{\lambda} \right)^n \right. \\ & \left. + C_{on}(\alpha) \left(\frac{\lambda}{\rho_c} \right)^{n+1} \right\} \left(\frac{1}{\sin \theta} \right) [n \cos \theta P_n^1(\cos \theta) \\ & - (n+1) P_{n-1}^1(\cos \theta)] = 0 \quad (19) \end{aligned}$$

The c subscripts indicate saddle point values.

Recalling the fact that only odd n coefficients are nonzero, one finds that every term on the right-hand side of Equation 19 contains a $\cos \theta$ factor. The right side of Equation 19 is, therefore, zero throughout the $\theta = \pi/2$ plane. In order to determine ρ_c , \bar{Y} must be eliminated between

Equation 18 and Equation 15 with $Q = -1$. This process yields
(for $\theta_c = \pi/2$)

$$0 = 1 + \frac{1}{\lambda \eta} \sum_{n=1}^{\infty} \frac{P_n^1(0)}{n(n+1)} \left\{ (n+1) \left(\frac{\rho_c}{\lambda} \right)^n [C_{in}(\beta) - C_{in}(\alpha)] - n \left(\frac{\lambda}{\rho_c} \right)^{n+1} C_{on}(\alpha) \right. \\ \left. + \frac{2 P_n^1(\cos \alpha)}{\cos \alpha} \left[- \left(\frac{\rho_c \sin \alpha}{\lambda} \right)^{n+1} + \left(\frac{\lambda}{\rho \sin \alpha} \right)^n \right] \right\} \quad (20)$$

Equation 20 may be solved by iteration for a self-consistent value of ρ_c . Finally, the ρ_c and θ_c values obtained may be used in Equation 15 for $Q = -1$ to compute the impact parameter \bar{y}_c which just closes the pass point to particles from infinity. \bar{y}_c is given by

$$\bar{y}_c = - \frac{\rho_c}{2} - \frac{\rho_c}{2 \lambda \eta} \sum_{n=1}^{\infty} \frac{P_n^1(0)}{n(n+1)} \left\{ [C_{in}(\beta) - C_{in}(\alpha)] \left(\frac{\rho_c}{\lambda} \right)^n \right. \\ \left. + C_{on}(\alpha) \left(\frac{\lambda}{\rho_c} \right)^{n+1} \right\} \quad (21)$$

A series of Störmer plots are given for a range of solenoid parameters in Figures 7 through 15. The range of parameters considered covers the useful range for shielding purposes. The solenoid radius is 0.048 Störmer units in Figures 7 and 8. For this radius, the Störmer plots are almost exactly like those for a dipole field. There is a slight distortion of the inner forbidden region for a long solenoid in Figure 8. The dipole analysis is completely adequate for $\lambda \ll 1$. Figure 3 may be used to convert the scales of these plots to lengths in meters for given particle energy and coil magnetic moment.

Figures 9, 10, and 11 are for coils with $\lambda = 0.086$ and with η/λ values of 0.25, 1.0 and 2.0, respectively. The differences between these plots and those for the dipole occur in the vicinity of the origin. The boundaries of the inner forbidden and inner allowed regions recede from

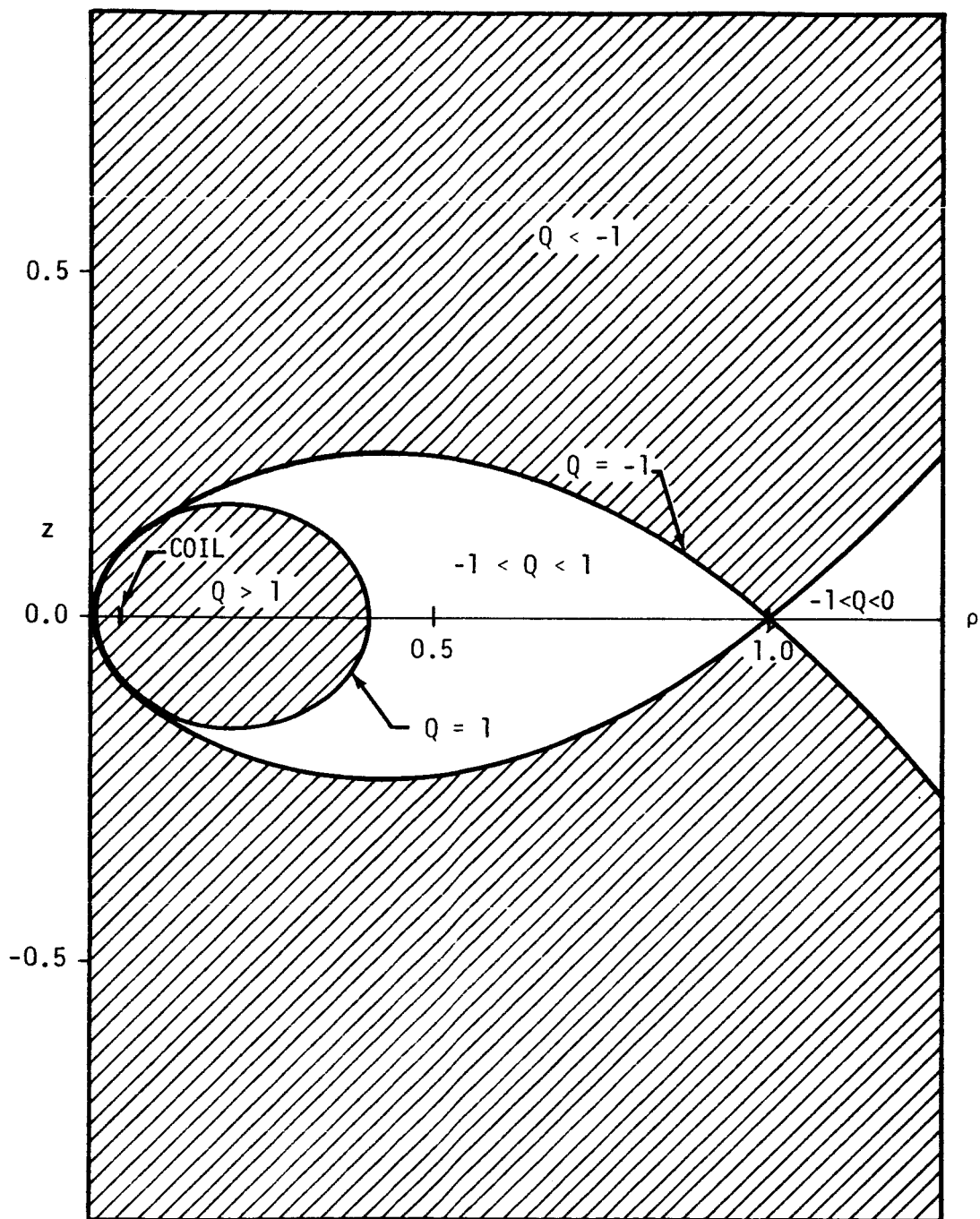


Figure 7. Allowed and Forbidden Regions of Charged Particle Motion About a Solenoid for $\bar{\gamma} = \bar{\gamma}_c$ ($\bar{\gamma} = -1.0004$, $\lambda = 0.048$, $\eta/\lambda = 0.25$)

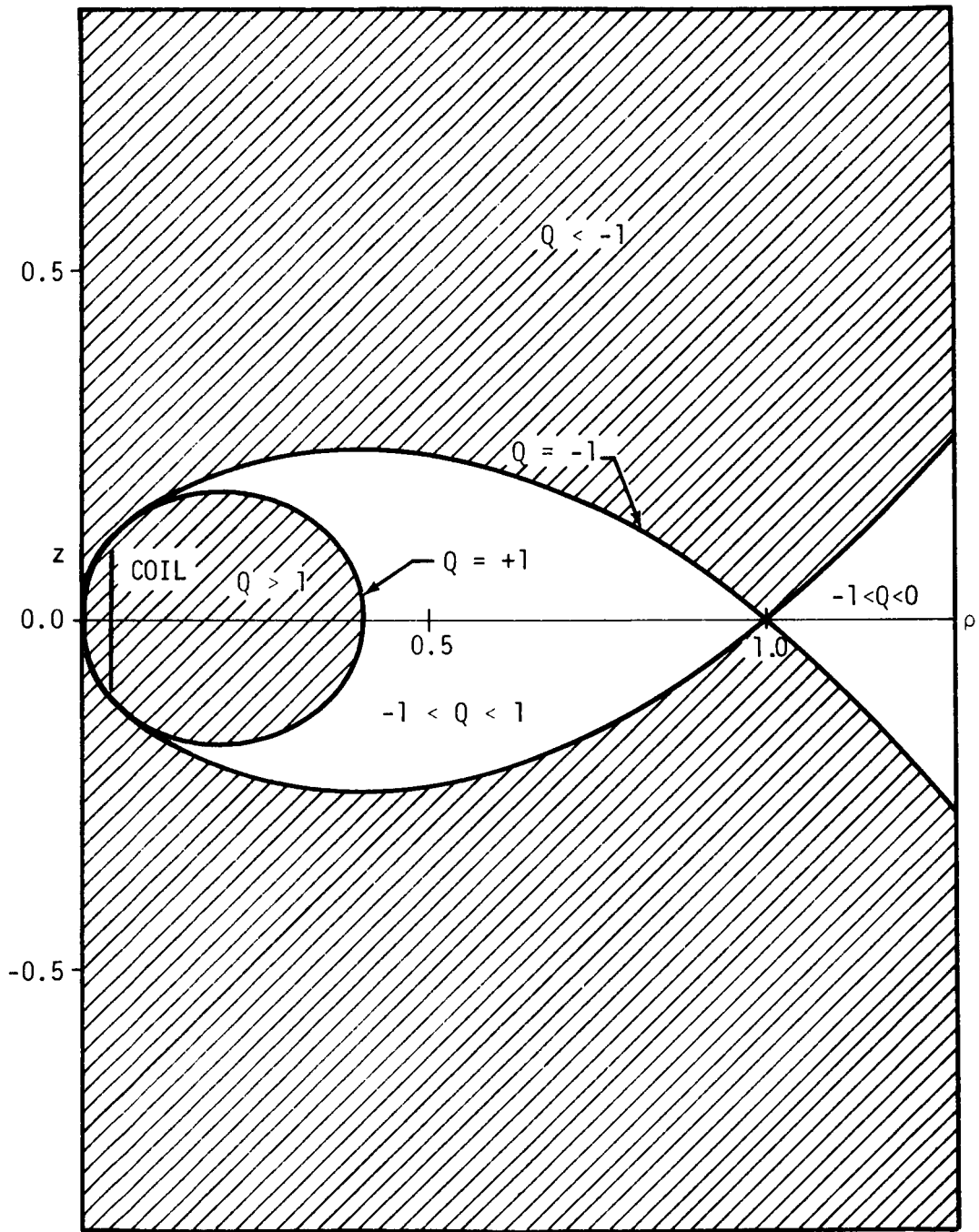


Figure 8. Allowed and Forbidden Regions of Charged Particle Motion About a Solenoid for $\bar{\gamma} = \bar{\gamma}_C$ ($\bar{\gamma} = -0.998$, $\lambda = 0.048$, $n/\lambda = 2$)

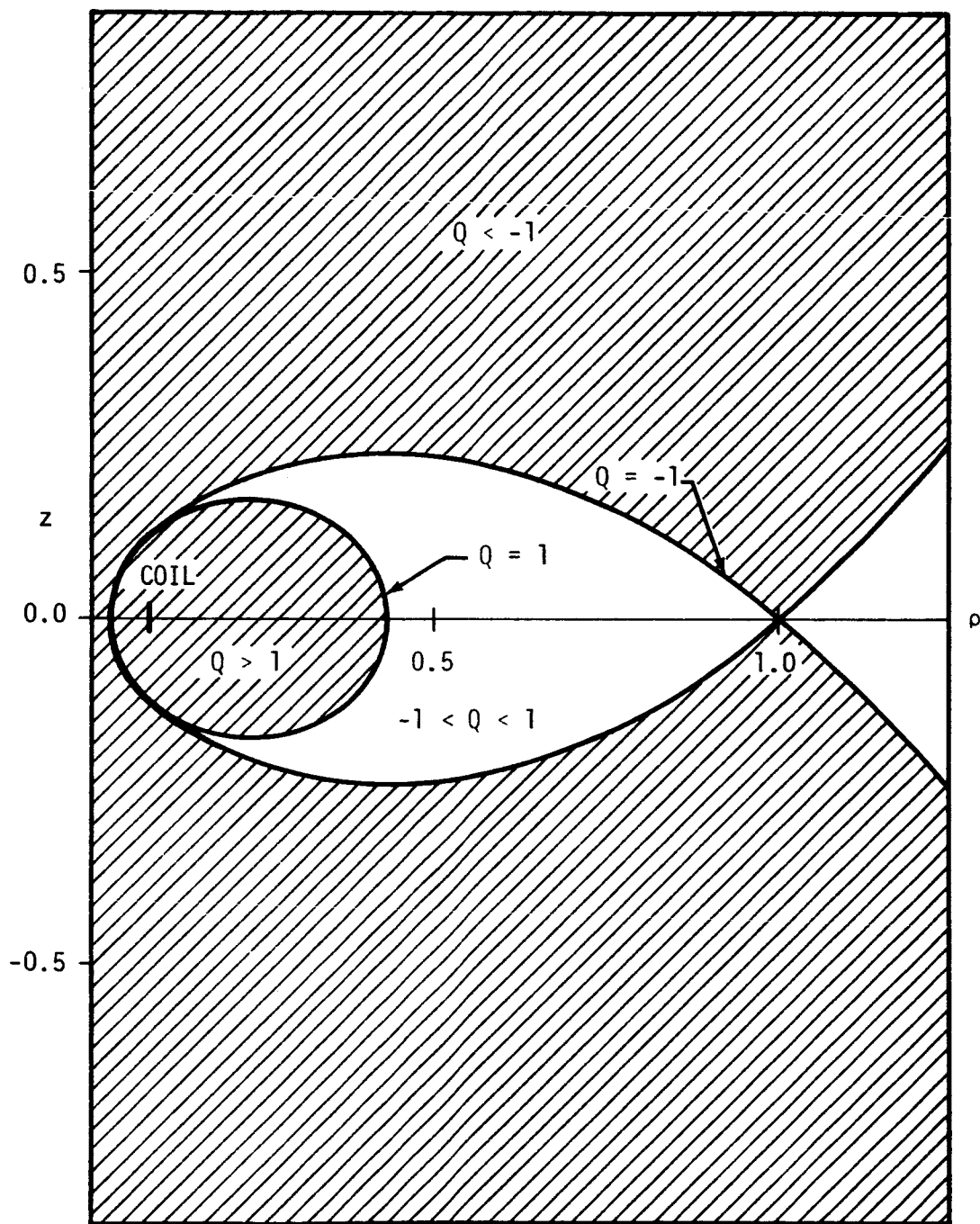


Figure 9. Allowed and Forbidden Regions of Charged Particle Motion About a Solenoid for $\bar{\gamma} = \bar{\gamma}_c$ ($\bar{\gamma} = -1.0013$, $\lambda = 0.086$, $\eta/\lambda = 0.25$)

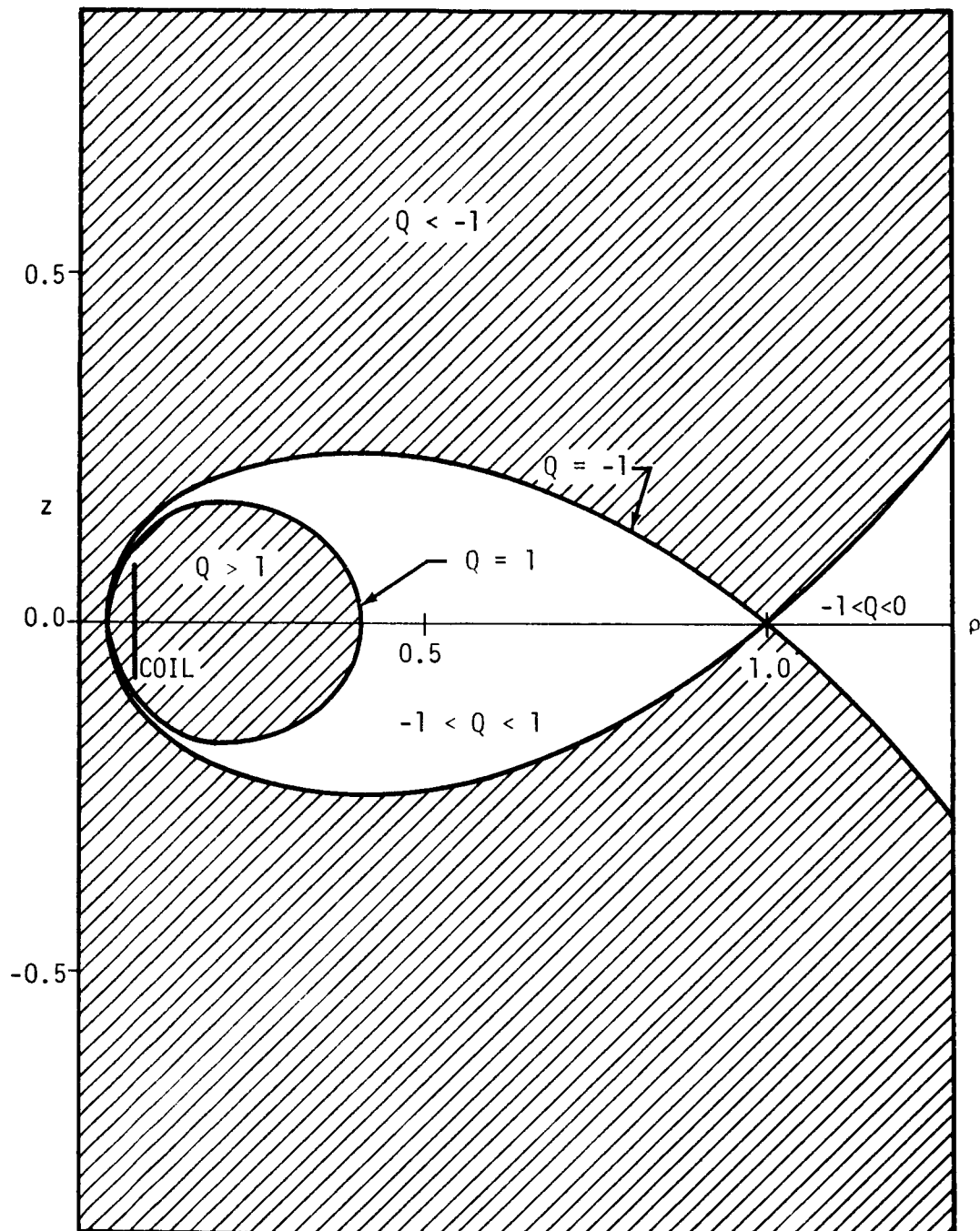


Figure 10. Allowed and Forbidden Regions of Unbound Charged Particle Motion About a Solenoid for $\bar{\gamma} = \bar{\gamma}_c$ ($\bar{\gamma} = -0.9995$, $\lambda = 0.086$, $\eta/\lambda = 1$)

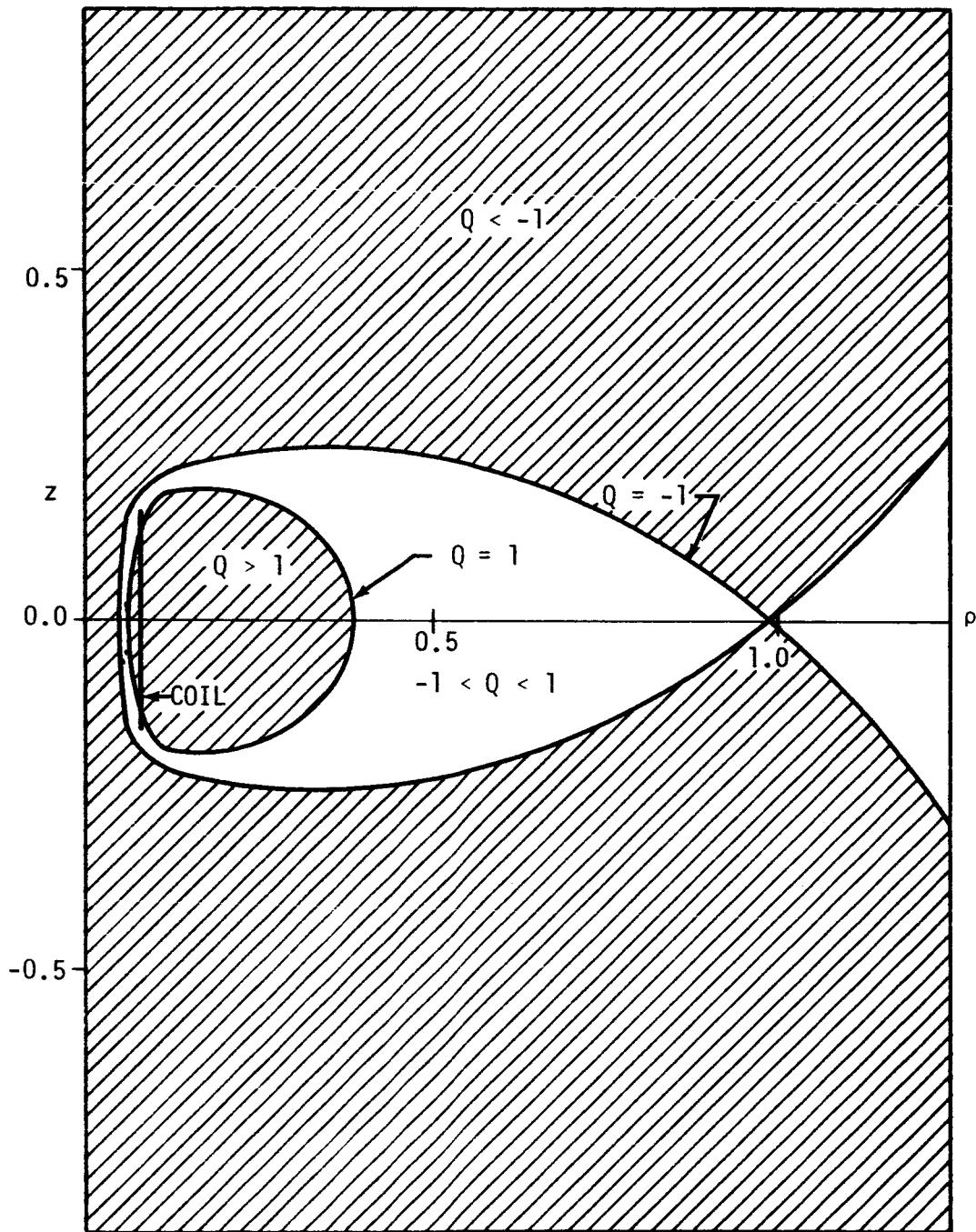


Figure 11. Allowed and Forbidden Regions of Unbound Charged Particle Motion About a Solenoid for $\bar{\gamma} = \bar{\gamma}_c$ ($\bar{\gamma} = -0.994$, $\lambda = 0.086$, $\eta/\lambda = 2$)

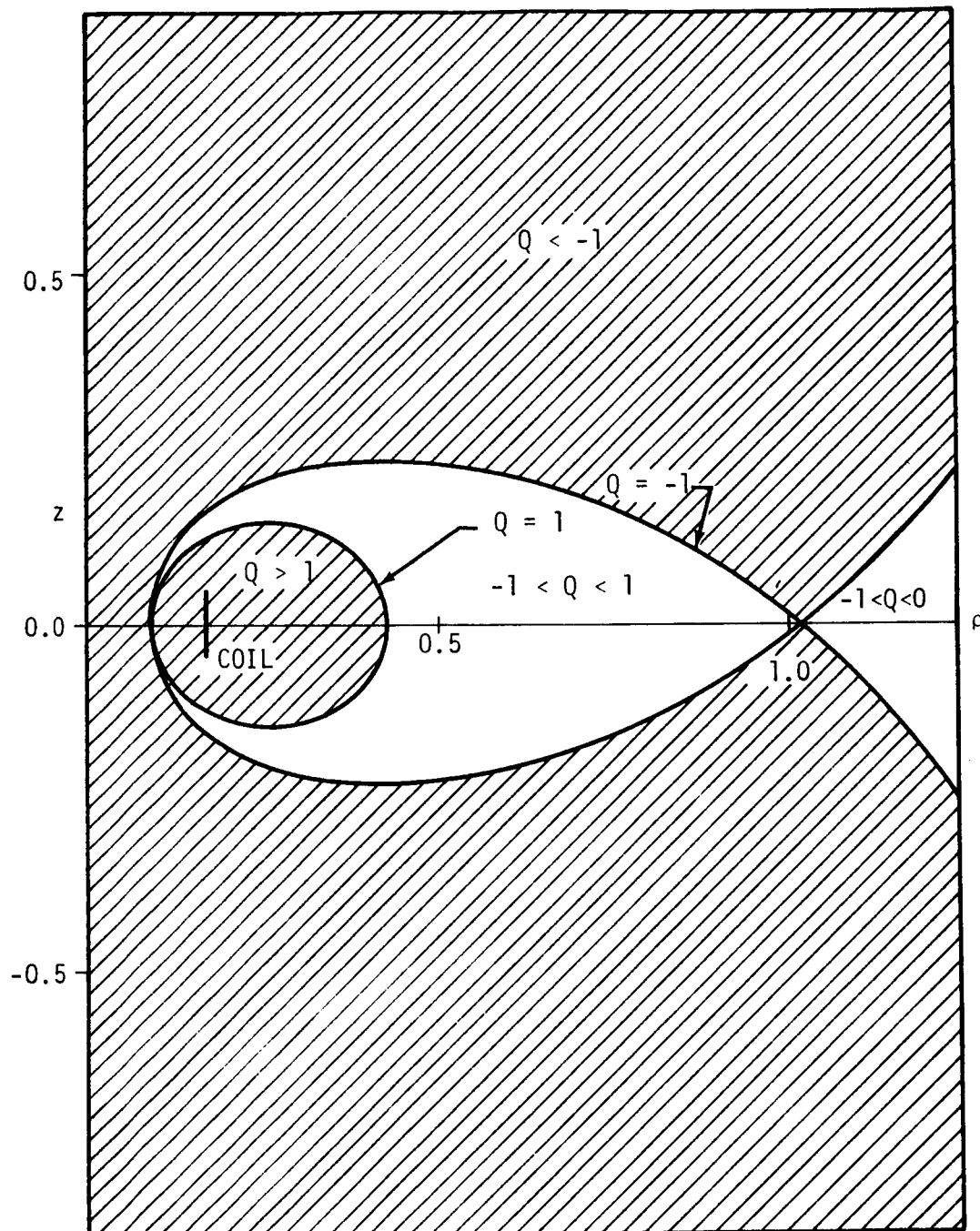


Figure 12. Allowed and Forbidden Regions of Unbound Charged Particle Motion in the Field of a Solenoid for $\bar{\gamma} = \bar{\gamma}_c$ ($\bar{\gamma} = -1.005$, $\lambda = 0.169$, $\eta/\lambda = 0.25$)

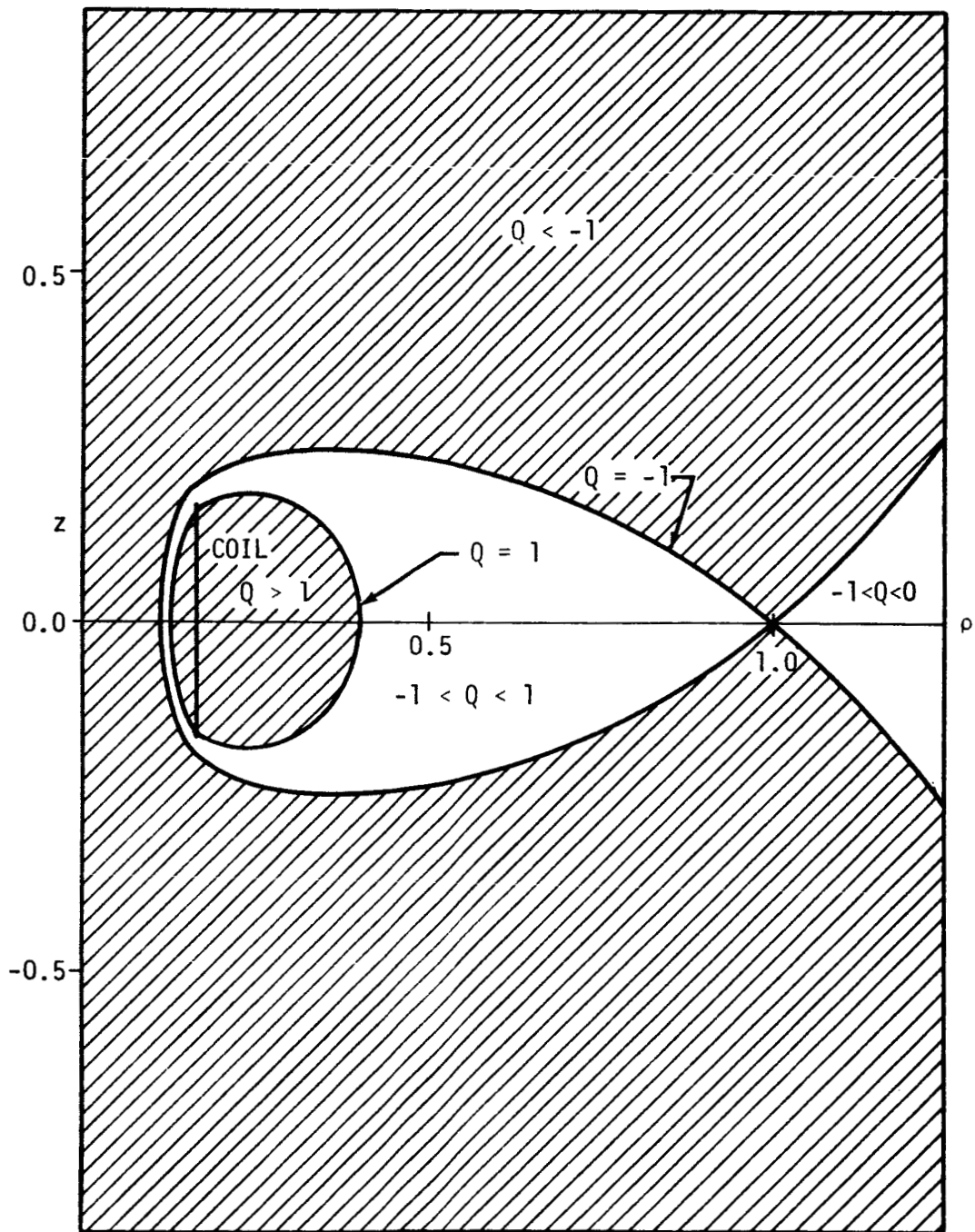


Figure 13. Allowed and Forbidden Regions of Unbound Charged Particle Motion in the Field of a Solenoid for $\bar{\gamma} = \bar{\gamma}_c$ ($\bar{\gamma} = -0.998$, $\lambda = 0.169$, $n/\lambda = 1$)

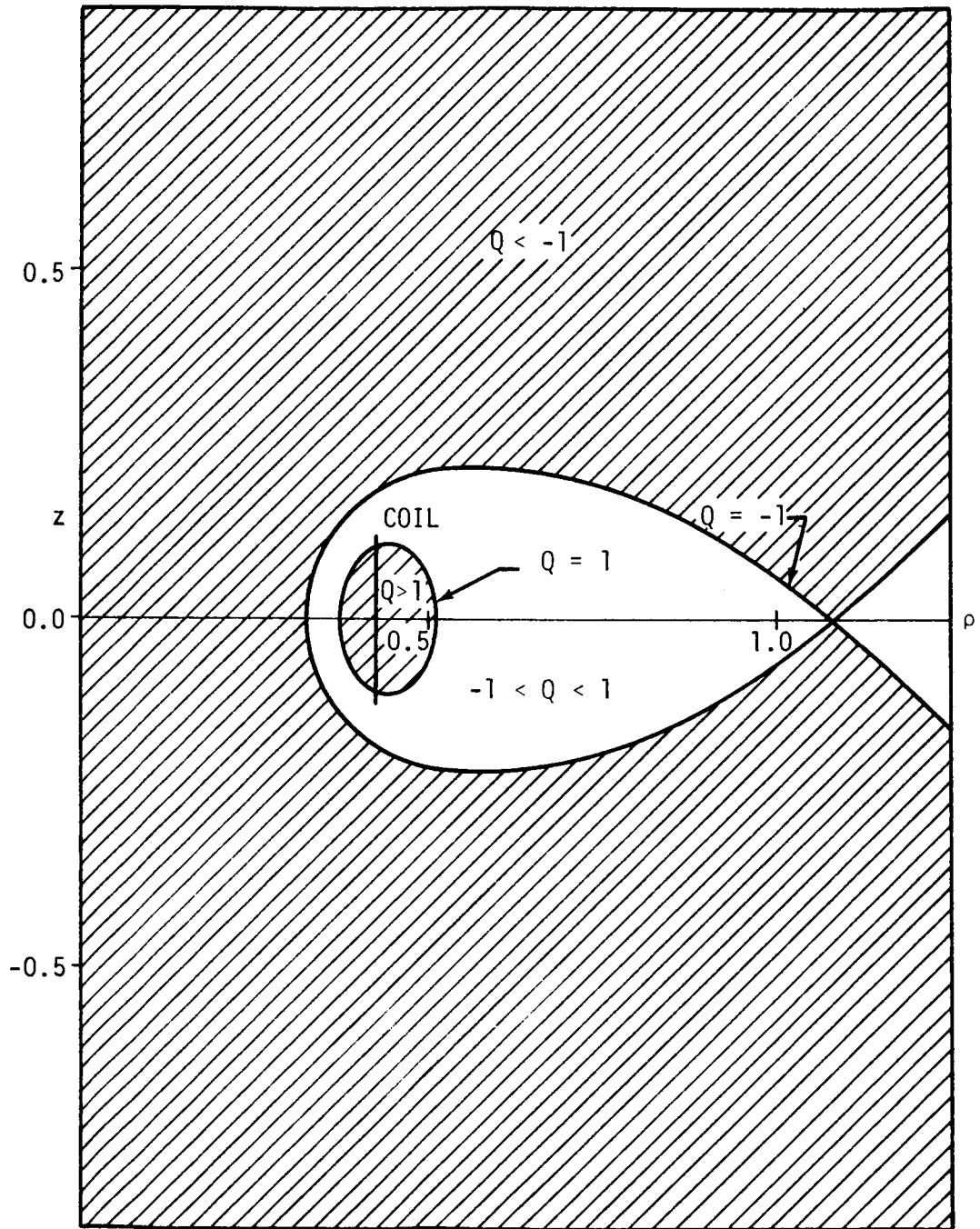


Figure 14. Allowed and Forbidden Regions of Unbound Charged Particle Motion in the Field of a Solenoid for $\bar{\gamma} = \bar{\gamma}_c$ ($\bar{\gamma} = -1.030$, $\lambda = 0.427$, $\eta/\lambda = 0.25$)

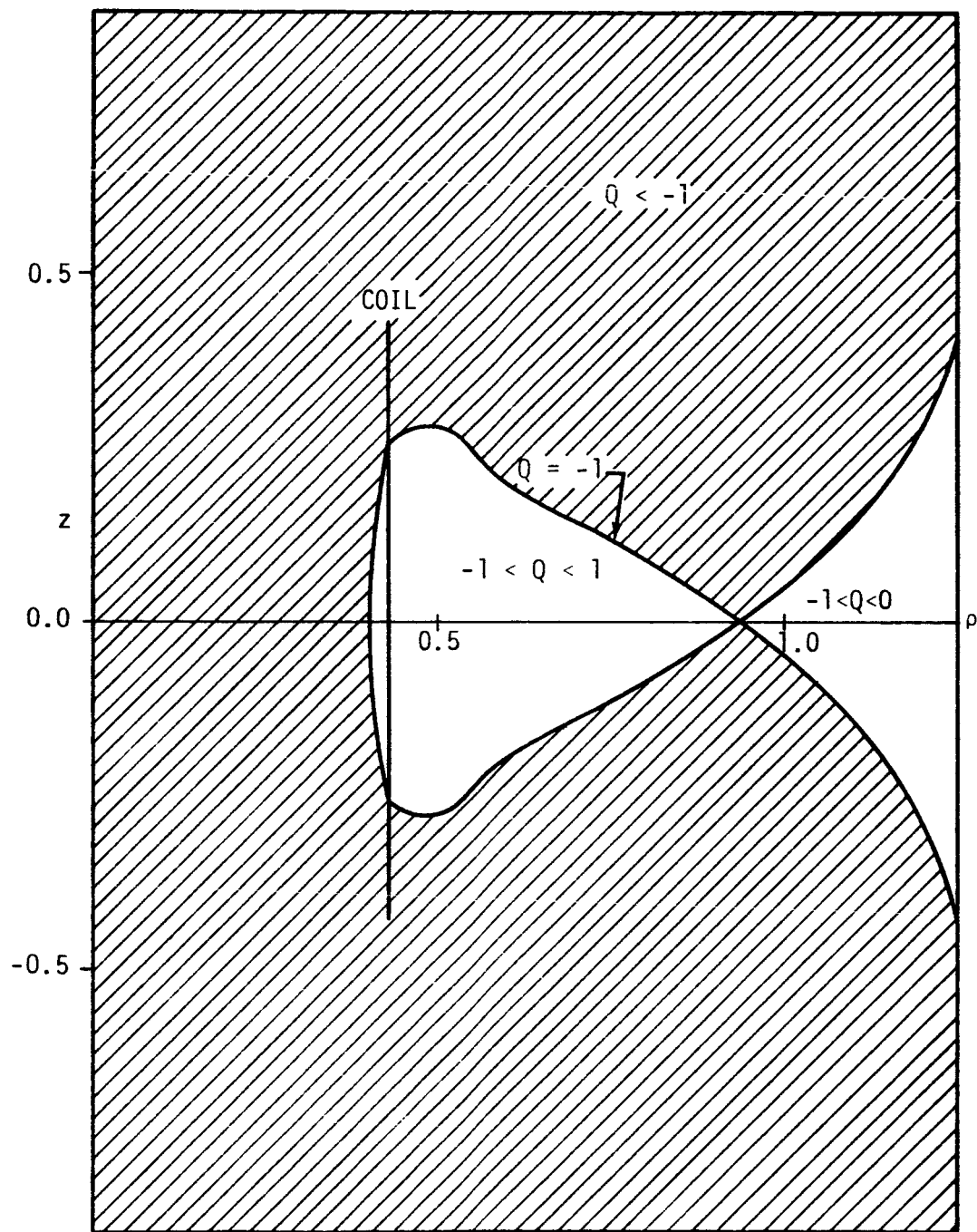


Figure 15. Allowed and Forbidden Regions of Unbound Charged Particle Motion in the Field of a Solenoid for $\bar{\gamma} = \bar{\gamma}_C$ ($\bar{\gamma} = -0.983$, $\lambda = 0.427$, $\eta/\lambda = 1$)

the origin toward the coil. The distortions of the inner forbidden and inner allowed regions increase as the length of the solenoid increases. An increase in λ corresponds to either an increase in particle kinetic energy or a decrease in magnetic moment of the coil and it is observed that the shielded region shrinks toward the inside of the coil with increasing particle energy. The region inside of the coil becomes exposed to radiation at lower particle energy than does the region immediately outside the coil.

Figures 12 and 13 show the allowed and forbidden regions for $\lambda = 0.169$ and for dimensionless lengths of 0.25 and 1.0, respectively. A further withdrawal of the shielded region from the center of the coil is observed and there is shrinkage and flattening of the shielded region toward the surface of the coil especially for the longer coils. It is also to be noted that the edges of the longer coils extend into the outer allowed regions. The effect of further increase of coil dimensionless radius, λ to 0.427 is shown in Figures 14 and 15. The completely shielded region still exists for the short coil ($\eta/\lambda = 0.25$) but the completely shielded region has disappeared for $\eta/\lambda = 1$. The shielded region has decreased in cross-sectional area by an order of magnitude between Figures 12 and 14. These two figures may be considered as representing the same coil for two kinetic energies differing by a factor of ten. For a longer coil ($\eta/\lambda = 1$), Figure 14 shows that the partially shielded or inner allowed region is very distorted.

Figures 5 and 7 through 15 give the general shape of the shielded regions for solenoids of various lengths and radii in Störmer units. For space vehicle shielding the shape and location of the shielded region are of great importance.

SHIELDING EFFECTIVENESS

The shielding effectiveness at any point in the magnetic field can be calculated for an isotropic flux of particles at large distances from the solenoid. The effectiveness of the magnetic shielding at point \vec{r} for particles of energy E may be defined as

$$\mathcal{E}(\vec{r}, E) \equiv 1 - \frac{\Phi(\vec{r}, E)}{\Phi(\vec{r}_\infty, E)}$$

where $\Phi(\vec{r}, E)$ is the flux of particles with energy E at the point \vec{r} and $\Phi(\vec{r}_\infty, E)$ is the flux of particles of this energy at infinity which is assumed to be isotropic and uniform spacewise.

The particle population is described in six-dimensional phase space defined by the position vector \vec{r} and the velocity vector \vec{v} by a distribution function $f(\vec{r}, \vec{v})$. Liouville's theorem states that the distribution function $f(\vec{r}, \vec{v})$ is constant along a particle trajectory in the six-dimensional space (Swann²¹). Swann has shown that a restricted form of Liouville's theorem^{13, 14, 17, 22} may be used in cosmic ray problems which require the distribution to be constant along a particle trajectory in real space.

The flux of particles with energy E at \vec{r} is related to the distribution function by

$$\Phi(\vec{r}, E) = \int_{\Omega} v f(\vec{r}, v) d\Omega$$

where Ω is the solid angle containing all directions from which particles may arrive at the point \vec{r} from infinity. It is assumed that v , p , and E are constant along a trajectory. Using the result of Liouville's theorem that

$$v f(\vec{r}, v) = v f(\vec{r}_\infty, v) \quad ,$$

the following equation is obtained for the particle flux at infinity

$$\Phi(r_\infty, E) = \int_{\Omega_\infty} v f(r, v) d\Omega \quad .$$

The ratio of particle flux at \vec{r} to the flux at infinity which is assumed to be isotropic is (Prescott^{13, 17})

$$\frac{\Phi(\vec{r}, E)}{\Phi(\vec{r}_\infty, E)} = \frac{\int_{\Omega} d\Omega}{\int_{\Omega_\infty} d\Omega} = \frac{\int \sin \omega d\omega d\delta}{4\pi} \quad .$$

Fermi¹⁴ has shown that the flux is uniform over the Störmer cone which gives the allowed directions of arrival at \vec{r} . Therefore,

$$\begin{aligned} \frac{\Phi(\vec{r}, E)}{\Phi(\vec{r}_\infty, E)} &= \frac{2\pi}{4\pi} \int_{\omega_1(\vec{r})}^{\omega_2(\vec{r})} \sin \omega d\omega \\ &= \frac{1}{2} [Q_1(\vec{r}) - Q_2(\vec{r})] \quad . \end{aligned}$$

The Störmer cone with half angle $\cos^{-1} Q$ is completely closed at $Q = +1$ and completely opened at $Q = -1$ thus,

$$\begin{aligned} \frac{\Phi(\vec{r}, E)}{\Phi(\vec{r}_\infty, E)} &= 0 \text{ if } Q_c \geq +1; \\ &= \frac{1}{2} (1 - Q_c) \text{ if } -1 < Q \leq 1 \text{ and } \rho < \rho_c; \\ &= 1 \text{ if } Q_c < -1 \text{ or if } -1 < Q < 0 \text{ and } \rho > \rho_c; \end{aligned}$$

where $Q_c = Q(\vec{r}_c)$.

Using this analysis, the shielding effectiveness for a given particle energy at any point in the magnetic field of the solenoid can be predicted.

A plot of contours of constant shielding effectiveness is given in Figure 16. The calculations were made for protons of kinetic energy 5 BeV and coil parameters $\mu_0 M = 10^4$ Wb-m, $R=2$ m, $L=1$ m but the results have more general application through the Störmer transformation. It is typical that the shielding effectiveness drops off very rapidly when going from the totally shielded region to the unshielded region and the shielding effectiveness of more than half the partially shielded region is less than 20 percent. Compared to the totally shielded region there is, however, a substantial part of the partially shielded region which offers good shielding.

Totally shielded and partially shielded volumes were numerically integrated for the three length-to-radius ratios considered for a range of coil radii in Störmer units. The results are given in Figure 17 where the totally shielded and partially shielded volumes in units of $(C_{st})^3$ are shown as a function of the coil radius, λ , in units of C_{st} . Figure 3 may be used to obtain a conversion factor to get the volumes in cubic meters. It is seen from Figure 17 that the shielded volumes for the three coils converge to the shielded volume for a dipole¹³ as $\lambda \rightarrow 0$. It is also to be noted that the smaller the length of the coil, the greater the totally shielded volumes (if radius and magnetic moment are the same). The totally shielded volume disappears earlier for larger η/λ as λ increases.

The exact manner in which the partially shielded volumes approach zero with increasing λ was not determined, but it was observed that the shielding effectiveness in the partially shielded region drops rapidly with increasing λ after the disappearance of the totally shielded region.

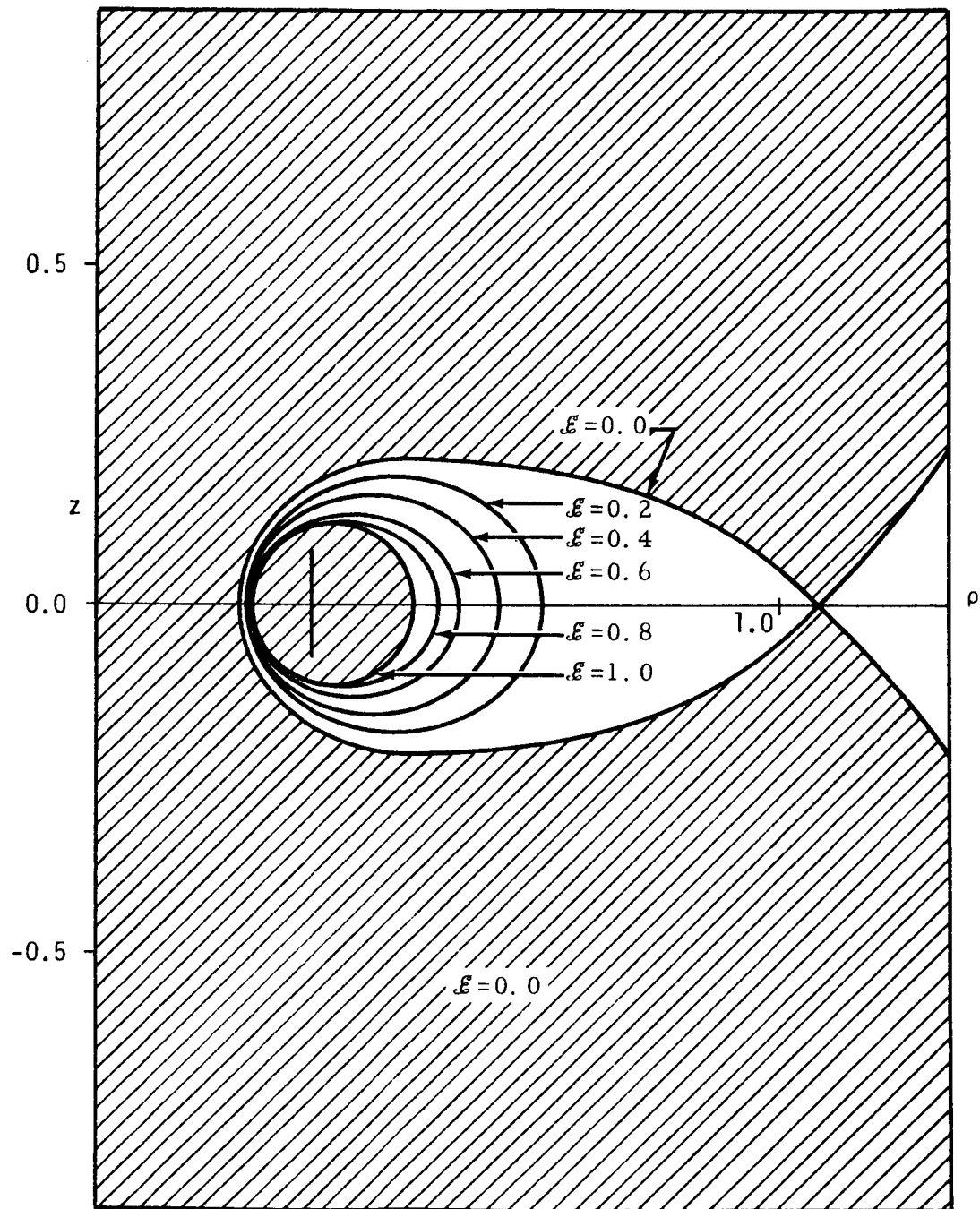


Figure 16. Shielding Effectiveness in the Partially Shielded Region of a Solenoid ($\lambda = 0.314$, $\eta/\lambda = 0.25$)

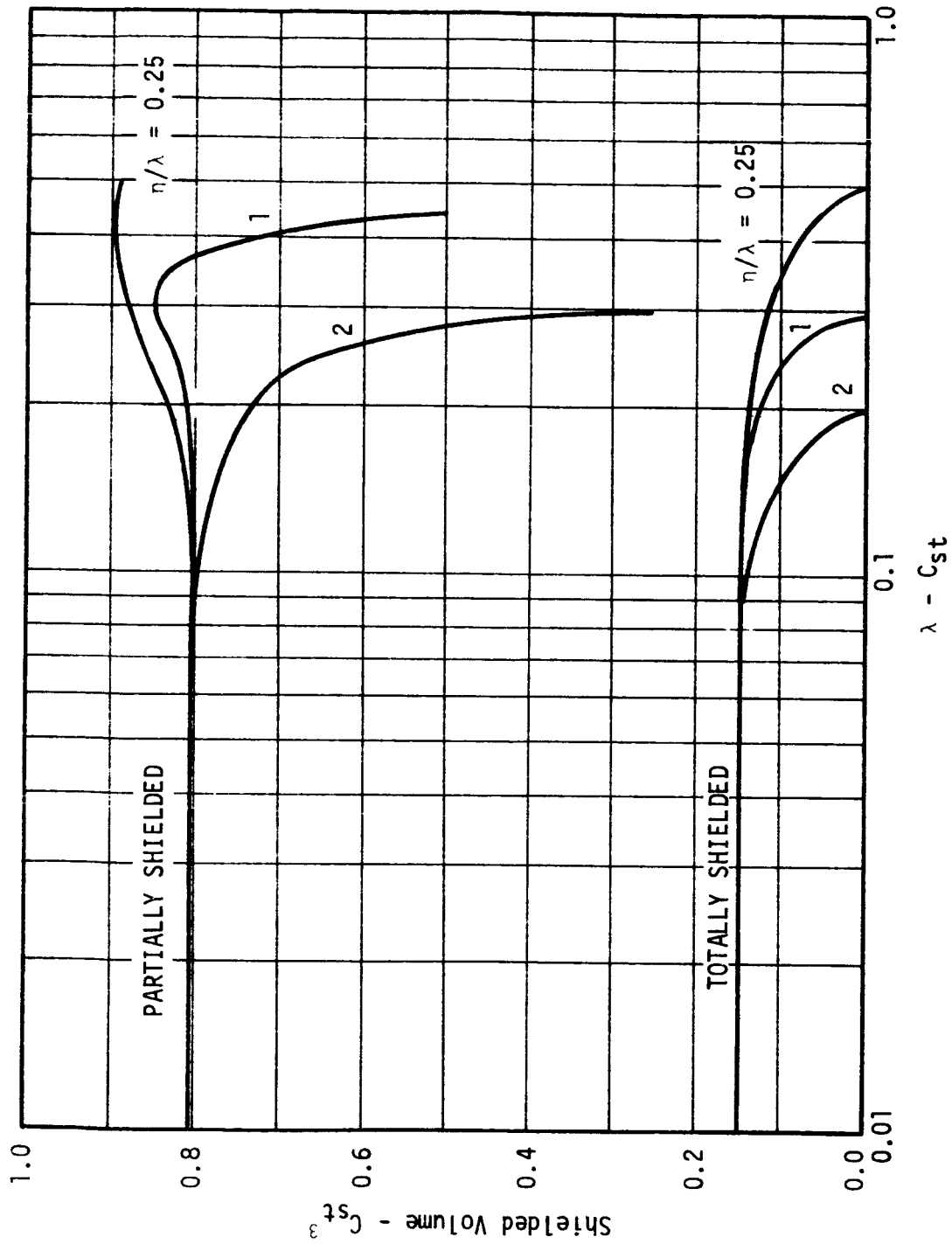


Figure 17. Totally Shielded and Partially Shielded Volumes for the Right Circular Solenoid as a Function of Coil Radius

CONCLUSIONS

The right circular solenoid is an interesting system for generating magnetic fields to shield spacecraft. The analysis has revealed significant departures from the shielding characteristics of the magnetic dipole for coil radii greater than about $0.15 C_{st}$ and lengths greater than about $0.3 C_{st}$. The shielded volume afforded by a coil of given radius and magnetic moment is maximized by making the coil as short as possible. A short coil may not, however, provide the largest useable shielded volume.

The major portions of the shielded volumes are located outside of the coil instead of inside. The implication is that the coil radius should be considerably less than the spacecraft radius in order to utilize the shielded volume.

Concentric solenoid configurations are of greater interest than a single solenoid since a combination of two solenoids can provide a field-free region for personnel and equipment between the two solenoids. The extension of the analysis of this report to a concentric pair of solenoids is rather simple, and the Störmer theorem for such a field configuration can be expressed in the form

$$Q = \frac{2\bar{Y}}{\rho \sin \theta} + \sum_{j=1}^2 \frac{m_j}{\lambda_j \eta_j} \sum_{n=1}^{\infty} \frac{P_n^1(\cos \theta)}{n(n+1)} \left\{ [C_{in}(\beta_j) - C_{in}(\alpha_j)] \left(\frac{\rho}{\lambda_j}\right)^n + C_{on}(\alpha_j) \left(\frac{\lambda_j}{\rho}\right)^{n+1} \right\}$$

where $m_1 = 1$ and $m_2 = \frac{M_2}{M_1}$ if the Störmer unit of length is defined in terms of M_1 and the subscripts $j = 1$ and 2 refer to the inner and outer solenoids. From the experience gained from the study of the combination field of the dipole and ring current²³, it is anticipated that for a range of particle energies two saddle points may be found in the Q surface with one falling

between the two solenoids and the other outside the outer solenoid. However, for appropriate magnetic moments and up to a certain particle energy there should be totally shielded and partially shielded volumes between the two solenoids. An analysis of the concentric solenoid configuration should be of considerable interest as the design of magnetic shields progresses.

REFERENCES

1. Dow, N. F., et al., "Evaluations of Space Vehicle Shielding", General Electric, TISR62SD31, 1962
2. Tooper, R. F. and W. O. Davies, "Electromagnetic Shielding of Space Vehicles", IAS Paper No. 62-156, 1962
3. Kash, S. W. and R. F. Tooper, "Active Shielding for Manned Spacecraft", *Astronautics*, pp. 68-75, September 1962
4. Levy, R. H., "Radiation Shielding of Space Vehicles by Means of Superconducting Coils", AVCO RR106, 1961
5. Levy, R. H., "The Prospects for Active Shielding", AVCO AMP-94, 1962
6. Brown, G. V., "Magnetic Radiation Shielding", *Proceedings of Conference on High Magnetic Fields*, (Kolm, editor), MIT Press, 1962
7. Bhattacharjie, A. and I. Michael, "Mass and Magnetic Dipole Shielding Against Electrons of the Artificial Radiation Belt", *AIAA J.* 2, 12 (1964)
8. Tooper, R. F., "Electromagnetic Shielding Feasibility Study" Wright Patterson AFB, ASD-TDR-63-194, 1963
9. Benedikt, E. J., "Cosmic Radiation Shielding of Space Vehicles by Axially Symmetric Electric Currents", North American Aviation, SID 64-387, AD459-262, 1964
10. Cladis, J. B., et al., "Feasibility of Magnetic Orbital Shielding System", Lockheed Missiles and Space Company, Technical Report 8-94-64-2, 1964
11. McDonald, P. F., "An Annotated Bibliography on Motion of Charged Particles in Magnetic Fields and Magnetic Shielding Against Space Radiation", Brown Engineering Company, Inc., Technical Note R-161, 1965
12. Störmer, Carl, The Polar Aurora, Oxford University Press, London, 1955

13. Prescott, A. D., "Distribution of Unbound Charged Particles in the Static Magnetic Field of a Dipole", NASA TMX-51312, 1964
14. O'Rear, Jay, et al. Nuclear Physics, A Course Given by Enrico Fermi, University of Chicago Press, Chicago, 1950
15. Urban, E. W., "Critical Störmer Conditions in Quadrupole and Double Ring-Current Fields", J. Math. Phys. 6, 12 (1965)
16. Stern, David, "The Vector Potential and Motion of Charged Particles in Axisymmetric Magnetic Fields", J. Geophys. Res. 69, 13 (1964)
17. Prescott, A. D., E. W. Urban, and R. D. Shelton, "The Application of the Liouville Theorem to Magnetic Shielding Problems", Second Symposium on Protection Against Radiations in Space, Gatlinburg, Tennessee, October 12-14, 1964, NASA SP-71, p. 189
18. Urban, E. W., "Charged Particle Motion in Axially Symmetric Magnetic Fields", Master's Thesis, University of Alabama, 1963
19. Smythe, W. R., Static and Dynamic Electricity, McGraw-Hill Book Company, Inc., New York, 1950
20. Ray. E. C., "Effects of a Ring Current on Cosmic Radiation", Phys. Rev. 101, 3 (1956)
21. Swann, W. F. G., "Application of Liouville's Theorem to Electron Orbits in the Earth's Magnetic Field", Phys. Rev. 44, 224 (1933)
22. Ray. E. C., "On the Application of Liouville's Theorem to the Intensity of Radiation Trapped in the Geomagnetic Field", State University of Iowa, SUI-59-21, 1959
23. McDonald, P. F., "Effect of the Ring Current on the Distribution of Unbound Particles in the Magnetosphere", Brown Engineering Company, Inc., Technical Note R-204, June 1966

APPENDIX A

COEFFICIENTS FOR EXPANSION OF THE VECTOR POTENTIAL

CENTRAL FIELD

$$C_{i1}(\beta) = 2 \cos \beta$$

$$C_{i3}(\beta) = -3 \cos \beta \sin^4 \beta$$

$$C_{i5}(\beta) = \frac{1}{4} [35 \cos^9 \beta - 120 \cos^7 \beta + 150 \cos^5 \beta \\ - 80 \cos^3 \beta + 15 \cos \beta]$$

$$C_{i7}(\beta) = \frac{1}{8} [-35 \cos \beta + 350 \cos^3 \beta - 1281 \cos^5 \beta \\ + 2324 \cos^7 \beta - 2261 \cos^9 \beta + 1134 \cos^{11} \beta \\ - 231 \cos^{13} \beta]$$

$$C_{i9}(\beta) = \frac{1}{64} [315 \cos \beta - 5040 \cos^3 \beta + 29484 \cos^5 \beta \\ - 89280 \cos^7 \beta + 158490 \cos^9 \beta - 172080 \cos^{11} \beta \\ + 112860 \cos^{13} \beta - 41184 \cos^{15} \beta + 6435 \cos^{17} \beta]$$

$$C_{i11}(\beta) = \frac{1}{128} [-693 \cos \beta + 16170 \cos^3 \beta - 136521 \cos^5 \beta \\ + 605880 \cos^7 \beta - 1632730 \cos^9 \beta + 2855292 \cos^{11} \beta \\ - 3326730 \cos^{13} \beta + 2572856 \cos^{15} \beta \\ - 1271985 \cos^{17} \beta + 364650 \cos^{19} \beta \\ - 46189 \cos^{21} \beta]$$

$$C_{in}(\beta) = 0 \quad n = 2, 4, 6, 8, 10, \text{ etc.}$$

REMOTE FIELD

$$C_{01}(\beta) = 2 \cot \beta$$

$$C_{03}(\beta) = \frac{4 \cos \beta}{\sin^3 \beta} - 7 \cot \beta$$

$$C_{05}(\beta) = \frac{6 \cos \beta}{\sin^5 \beta} - \frac{27 \cos \beta}{\sin^3 \beta} + \frac{99 \cot \beta}{4}$$

$$C_{07}(\beta) = \frac{8 \cos \beta}{\sin^7 \beta} - \frac{66 \cos \beta}{\sin^5 \beta} + \frac{143 \cos \beta}{\sin^3 \beta} - \frac{715 \cot \beta}{8}$$

$$C_{09}(\beta) = \frac{10 \cos \beta}{\sin^9 \beta} - \frac{130 \cos \beta}{\sin^7 \beta} + \frac{975 \cos \beta}{2 \sin^5 \beta} - \frac{5525 \cos \beta}{8 \sin^3 \beta} \\ + \frac{20995 \cos \beta}{64 \sin \beta}$$

$$C_{011}(\beta) = \frac{12 \cos \beta}{\sin^{11} \beta} - \frac{225 \cos \beta}{\sin^9 \beta} + \frac{1275 \cos \beta}{\sin^7 \beta} - \frac{24225 \cos \beta}{8 \sin^5 \beta} \\ + \frac{101745 \cos \beta}{32 \sin^3 \beta} - \frac{156009 \cos \beta}{128 \sin \beta}$$

$$C_{0n}(\beta) = 0 \quad n = 2, 4, 6, 8, 10, \text{ etc.}$$

APPENDIX B
COMPUTER PROGRAM

PRINCIPAL FORTRAN VARIABLES

<u>Variable</u>	<u>Description</u>
AL	L - length of solenoid (m)
AR	R - radius of solenoid (m)
BETA	$\beta - \tan^{-1} \frac{2R}{L}$
CQ	Value of Q for which allowed cone is completely closed (Q = +1)
CST	C _{st} - Störmer unit of length (m)
DMM	$\mu_0 M$ - magnetic moment of solenoid (Wb-m)
DT	$\Delta \theta$ - increment of θ (deg)
ENK	Kinetic energy (eV)
ENR	Rest energy (eV)
GA	$\bar{\gamma}$ (see Equation B-8)
PL	$P_n^1(\cos \theta)$ - Legendre polynomial
Q	See Equation B-9
QA	Q = ±1
RA	ρ at Q = ±1 (boundary of a forbidden region)
RHO	ρ
RT	ρ_c - see Equation B-7
T	θ - initial angle (deg)
TN	θ_f - final angle (deg)

<u>Variable</u>	<u>Description</u>
VP	Partially shielded volume (C_{st}^3)
VT	Totally shielded volume (C_{st}^3)
XL	λ

PROGRAM DESCRIPTION

A computer program was written in FORTRAN to study the shielding characteristics of magnetic fields generated by right circular solenoids. The quantities E_k , E_R , $\mu_0 M$, R , CQ , θ_i , $\Delta\theta$, θ_f , and L are input and the following quantities are computed:

$$C_{st} = \frac{(c \mu_0 M)^{\frac{1}{2}}}{2 \sqrt{\pi} (E_k^2 + 2 E_k E_R)^{0.25}} \quad (B-1)$$

where

c - speed of light (m/sec) .

$$\lambda = \frac{R}{C_{st}} \quad (B-2)$$

$$\beta = \tan^{-1} \frac{2R}{L} \quad (B-3)$$

$$\begin{aligned} \alpha &= \pi/2 \text{ if } r < R \\ &= \beta \text{ if } r > R/\sin \beta \\ &= \sin^{-1} (R/r) \text{ if } R < r < R/\sin \beta \end{aligned} \quad (B-4)$$

$$\eta = L/2 C_{st} \quad (B-5)$$

$$\rho = r/C_{st} \quad (B-6)$$

$$0 = 1 + \frac{1}{\lambda\eta} \sum_{n=1}^{11} \frac{P_n^1(0)}{n(n+1)} \left\{ (n+1) \left(\frac{\rho_c}{\lambda}\right)^n [C_{in}(\beta) - C_{in}(\alpha)] - n \left(\frac{\lambda}{\rho_c}\right)^{n+1} C_{on}(\alpha) + \frac{2 P_n^1(\cos \alpha)}{\cos \alpha} \left[\left(\frac{\lambda}{\rho_c \sin \alpha}\right)^n - \left(\frac{\rho_c \sin \alpha}{\lambda}\right)^{n+1} \right] \right\} \quad (B-7)$$

Using the quantities computed in Equations B-1 through B-6, Equation B-7 is solved by iteration for ρ and the value of ρ which satisfies Equation B-7 is denoted by ρ_c . Using this value the following expression is evaluated.

$$\bar{V}_c = -\frac{\rho_c}{2} - \frac{\rho_c}{2\lambda\eta} \sum_{n=1}^{11} \frac{P_n^1(0)}{n(n+1)} \left\{ [C_{in}(\beta) - C_{in}(\alpha)] \left(\frac{\rho_c}{\lambda}\right)^n + C_{on}(\alpha) \left(\frac{\lambda}{\rho_c}\right)^{n+1} \right\} \quad (B-8)$$

Using the quantity \bar{V}_c ,

$$Q = \frac{2\bar{V}_c}{\rho \sin \theta} + \frac{1}{\lambda\eta} \sum_{n=1}^{11} \frac{P_n^1(\cos \theta)}{n(n+1)} \left\{ [C_{in}(\beta) - C_{in}(\alpha)] \left(\frac{\rho}{\lambda}\right)^n + C_{on}(\alpha) \left(\frac{\lambda}{\rho}\right)^{n+1} \right\} \quad (B-9)$$

Q is evaluated for values of θ and incremented values of ρ . Values of Q are examined to determine the flux.

$$\begin{aligned} \frac{\Phi(\vec{r}, E)}{\Phi(\vec{r}_\infty, E)} &= 0 \text{ if } Q_c \geq +1; \\ &= \frac{1}{2} (1 - Q_c) \text{ if } -1 < Q \leq 1 \text{ and } \rho < \rho_c; \\ &= 1 \text{ if } Q_c < -1 \text{ or if } -1 < Q < 0 \text{ and } \rho > \rho_c; \end{aligned} \quad (B-10)$$

where $Q_c = Q(\bar{\gamma}_c)$. Values of ρ are interpolated for at $Q = \pm 1$. The quantities in Equation B-9 and B-10 are computed over the specified range of θ . The values of θ and ρ are used to calculate the volume of the partially and totally shielded regions.

The program is written in seven parts; a main program and six subroutines. Their purpose is described below.

Main Program

The main program accepts input, evaluates Equations B-1 through B-6 and controls the iteration processes. It also computes the partially and totally shielded volumes and all data is output by the main program.

Subroutines

Subroutine COMC computes C_{in} and C_{on} for a specified angle. Subroutine LPOL computes the associated Legendre polynomials $P_1^1(\cos \theta)$ through $P_{11}^1(\cos \theta)$. Subroutine FPH evaluates the right-hand side of Equation B-7. Subroutine GAM evaluates Equation B-8. Subroutine QUE evaluates Equation B-9 and computes the radial and angular components of magnetic induction. Function FX evaluates Equation B-10.

Input

The following quantities are necessary input to the program.

<u>Variable</u>	<u>Description</u>	<u>Format</u>	<u>Card Column</u>
ENK	E_k - kinetic energy (eV)	E15.4	1-15
ENR	E_R - rest energy (eV)	E15.4	16-30
DMM	$\mu_o M$ - magnetic moment of the solenoid (Wb-m)	E15.4	31-45
AR	R - radius of the solenoid (m)	F5.2	46-50
CQ	Q value for closure of the allowed cone (CQ = 1 in all runs in this study)	F5.2	51-55

<u>Variable</u>		<u>Format</u>	<u>Card Column</u>
T	θ_i - initial angle (deg)	F5.2	56-50
DT	$\Delta\theta$ - increment for θ (deg)	F5.2	61-65
TN	θ_f - final value for θ (deg)	F5.2	66-70
AL	L - length of solenoid (m)	F5.2	71-75

Output

The following quantities are output with each run.

LAMBDA	λ
BETA	β (deg)
DMM	$\mu_o M$ (Wb-m)
AL	L (m)
ROOT	ρ_c
PHI	Equation 7 evaluated at ρ_c
GAMMA	$\bar{\gamma}_c$
ENK	E_k (eV)
ENR	E_R (eV)
CST	C_{st} (m)
THETA	θ (deg)
AR	R (m)
RHO	ρ
Q	Results of Equation 9
BR, BZ	Components of magnetic induction in cylindrical coordinates (Wb/m^2)

FLUX	Solution of Equation 10
Q1	± 1
R1	Interpolated value of ρ at $Q = \pm 1$
PARTIAL VOLUME	Volume of rotation of the partially shielded region in units of C_{st}^3
TOTAL VOLUME	Volume of rotation of the totally shielded region in units of C_{st}^3

COMPUTER PROGRAM LISTING

```
MAIN PROGRAM
DIMENSION THK(60),THD(60),RPA(60),RPB(60),RTA(60),RTB(60)
DIMENSION RHO(200),QXX(200),FLUX(200),QYY(200),RYY(200),RWW(200)
DIMENSION PL(11),PA(11),PO(11),COX(200,6),CIX(200,6),TCI(6),TCO(6)
DIMENSION BZ(200),BRR(200),COB(6),CIB(6)
COMMON TCI,TCO,PL,PA,PO,COX,CIX,COB,CIB,XL,XN,BE,SB,CB,SA,CA,CLN
COMMON F,G,H,BK,GA,RT,TO,ST,CT,BR,BT
P=3.14159265
CL=2.997925E+08
PO(1)=1.
PO(2)=-1.5
PO(3)=15./8.
PO(4)=-35./16.
PO(5)=315./128.
PO(6)=-693./256.
DO 98 I=1,200
PHI =0.
98 QYY(I)=0.
99 RT=0
100 READ(5,101)ENK,ENR,DMM,AR,CQ,T,DT,TN,AL
101 FORMAT(3E15.4,7F5.2)
IF (DT=.01) 999,999,102
102 BE=ATAN(AR*2./AL)
BETA=BE/.0174533
CALL COMC(BE)
DO 103 I=1,6
COB(I)=TCO(I)
103 CIB(I)=TCI(I)
IX=0
DO 104 I=1,60
RPA(I)=0.
RPB(I)=0.
RTA(I)=0.
104 RTB(I)=0.
CST=.5*SQRT(CL*DMM/P)/(ENK*ENK+2.*ENK*ENR)**.25
SB=SIN(BE)
CB=COS(BE)
XL=AR/CST
BK=DMM/(2.*P*AL*AR**2)
XN=AL/(2.*CST)
CLN=1./(XL*XN)
200 VF=XL+.05
CALL FPH(VF)
FF=F
VL=XL+3.
```

```

        CALL FPH(VL)
        FL=F
201  VM=.5*(VF+VL)
202  CALL FPH(VM)
        FM=F
203  IA=1
        IB=1
        IC=1
        IF (FF) 204,214,205
204  IA=-1
205  IF (FM) 206,215,207
206  IB=-1
207  IF (FL) 208,216,209
208  IC=-1
209  IF (ABS(IA+IB+IC) .GT. 2) GO TO 500
        IF ((VL-VF)-.005) 212,212,210
210  IF (IA .NE. IB) GO TO 211
        VF=VM
        FF=FM
        GO TO 201
211  VL=VM
        FL=FM
        GO TO 201
212  VZ=VF-(VM-VF)*FF/(FM-FF)+FF*FM/(FM-FF)
        1*((VL-VM)/(FL-FM)-(VM-VF)/(FM-FF))
213  RT=VZ
        CALL FPH(VZ)
        PHI=F
        CALL GAM(VZ)
        GA=G
        GO TO 500
214  VZ=VF
        GO TO 213
215  VZ=VM
        GO TO 213
216  VZ=VL
        GO TO 213
500  WRITE(6,501)
501  FORMAT(1H1,7X,6HLAMBDA,12X,4HBETA,13X,3HDMM,14X,2HAL,12X,4HROOT,
        113X,3HPHI,11X,5HGAMMA)
        WRITE(6,502)XL,BETA,DMM,AL,RT,PHI,GA
502  FORMAT(7E16.5)
        IF (RT) 601,99,601
601  RHO(1)=.05
        RWW(1)=.05/XL
        RN=1.5
        RI=.05
        N=IFIX((RN-.05)/.05)
        DO 605 J=2,N
        RHO(J)=RHO(J-1)+RI
        IF (XL-RHO(J)) 602,605,605

```

```

602 IF (XL/SB-RHO(J)) 605,605,603
603 U=RHO(J)/XL
      V=XL/RHO(J)
      ALP=ASIN(V)
      CALL COMC(ALP)
      DO 604 K=1,6
      COX(J,K)=TCO(K)
604 CIX(J,K)=TCI(K)
      CONTINUE
605 RWW(J)=RHO(J)/XL
606 SR=0
607 SQ=2
608 TO=T*.0174533
      ST=SIN(TO)
609 DO 617 I=1,N
      R=RHO(I)
610 CALL QUE(R,I)
      Q=H
      FLUX(I)=FX(Q,RT,R)
      QXX(I)=Q
      BRR(I)=BR*ST+BT*CT
      BZ(I)=BR*CT-BT*ST
      WQ=Q
      J=0
611 IF (CQ-ABS(WQ)) 612,615,613
612 J=J+1
613 J=J+2
      GO TO (615,614,614,616,615,616),J
614 WQ=SQ
      GO TO 611
615 QA=(SQ+Q)/ABS(SQ+Q)
      RA=SR+(QA-SQ)*(R-SR)/(Q-SQ)
      QYY(I)=QA
      RYY(I)=RA
616 SQ=Q
617 SR=R
      IX=IX+1
      J=IX
      THD(J)=T
      THK(J)=TO
      DO 809 I=2,200
      IF (RHO(I)-RT) 798,798,810
798 IF (I .GT. 2) GO TO 800
      IF (FLUX(1)) 800,799,800
799 RPA(J)=.0001
      RTA(J)=.0001
800 IF (ABS(FLUX(I)-FLUX(I-1))-0.999) 802,802,801
801 A=RHO(I-1)
      B=RHO(I)
      C=QXX(I-1)
      D=QXX(I)

```

```

      FSN=(B-A)/(D-C)
      RPT=A+(-1.-C)*FSN
      RTT=A+(1.-C)*FSN
      IF (RPA(J)) 1801,1801,1802
1801 RPA(J)=RPT
      RTA(J)=RTT
      GO TO 802
1802 RPB(J)=RPT
      RTB(J)=RTT
      802 IF (QYY(I)) 803,809,806
      803 IF (RPA(J)) 804,805,804
      804 RPB(J)=RYY(I)
      GO TO 618
      805 RPA(J)=RYY(I)
      GO TO 809
      806 IF (RTA(J)) 807,808,807
      807 RTB(J)=RYY(I)
      GO TO 809
      808 RTA(J)=RYY(I)
      809 CONTINUE
      810 IF (ABS(T-90.)-.01) 811,618,618
      811 RPB(J)=RT
      618 WRITE(6,619)
      619 FORMAT(/ /1H ,8X,3HENK,12X,3HENR,12X,3HCST,9X,3HDMM,6X,5HTHETA,5X,
      16HLAMBDA,6X,2HAL,8X,2HAR,4X,5HGAMMA,5X,4HROOT)
      WRITE(6,620)ENK,ENR,CST,DMM,T,XL,AL,AR,GA,RT
      620 FORMAT(3E15.8,6F10.2,6F10.3)
      WRITE(6,621)
      621 FORMAT(/ /1H ,8HRHO/RHO1,5H RHO,10X,1HQ,12X,2HBR,13X,2HBZ,12X,
      14HFLUX,13X,2HQ1,13X,2HR1)
      DO 625 I=1,N
      IF (QYY(I)) 624,622,624
      622 WRITE(6,623)(RWW(I),RHO(I),QXX(I),BRR(I),BZ(I),FLUX(I))
      623 FORMAT(1H ,2F8.5,4E15.5,5X,F8.5,E15.5)
      GO TO 625
      624 WRITE(6,623)(RWW(I),RHO(I),QXX(I),BRR(I),BZ(I),FLUX(I),RYY(I),
      1QYY(I))
      625 CONTINUE
      DO 626 I=1,N
      626 QYY(I)=0.
      T=T+DT
      IF (T-TN) 606,606,627
      627 IF ((T-DT)-TN) 628,629,629
      628 T=TN
      GO TO 606

      VP=0.
      VT=0.
      DO 909 I=1,K
      CT=SIN(THK(I))
      ST=COS(THK(I))

```

```

CX=SIN(THK(I+1))
SX=COS(THK(I+1))
IF (VP) 900,900,903
900 IF (RPA(I)) 909,909,901
901 IF (RPB(I)) 909,909,902
902 X1=RPA(I)*CT
DX=RPB(I)*CT-X1
XM=X1+.5*DX
VP=VP+2.*P*XM*DX*RPB(I)*ST
903 IF (VT) 904,904,907
904 IF (RTA(I)) 908,908,905
905 IF (RTB(I)) 908,908,906
906 X1=RTA(I)*CT
DX=RTB(I)*CT-X1
XM=X1+.5*DX
VT=VT+2.*P*XM*DX*RTB(I)*ST
907 X1=RTA(I+1)*CX
DX=RTA(I)*CT-X1
XM=X1+.5*DX
PV1=2.*P*XM*DX*.5*(RTA(I+1)*SX+RTA(I)*ST)
X1=RTB(I)*CT
DX=RTB(I+1)*CX-X1
XM=X1+.5*DX
VT=VT+PV1+2.*P*XM*DX*.5*(RTB(I+1)*SX+RTB(I)*ST)
908 X1=RPA(I+1)*CX
DX=RPA(I)*CT-X1
XM=X1+.5*DX
PV1=2.*P*XM*DX*.5*(RPA(I+1)*SX+RPA(I)*ST)
X1=RPB(I)*CT
DX=RPB(I+1)*CX-X1
XM=X1+.5*DX
VP=VP+PV1+2.*P*XM*DX*.5*(RPB(I+1)*SX+RPB(I)*ST)
909 CONTINUE
WRITE(6,910)
910 FORMAT(1H1,5X,5HTHETA,5X,23HPARTIAL SHIELDED REGION,5X,
12HTOTAL SHIELDED REGION)
DO 915 I=1,IX
IF (RPA(I)) 911,915,911
911 IF (RTA(I)) 914,912,914
912 WRITE(6,913)THD(I),RPA(I),RPB(I)
913 FORMAT(6X,F4.1,5X,2F10.4,8X,2F10.4)
GO TO 915
914 WRITE(6,913) THD(I),RPA(I),RPB(I),RTA(I),RTB(I)
915 CONTINUE
VP=2.*VP
VT=2.*VT
WRITE(6,916)VP,VT
916 FORMAT(//1H ,16HPARTIAL VOLUMN =E12.5,5X,14HTOTAL VOLUMN =E12.5)
GO TO 99
999 M=0
END

```

```

SUBROUTINE COMC(ANG)
DIMENSION PL(11),PA(11),PO(11),COX(200,6),CIX(200,6),TCI(6),TCO(6)
DIMENSION COB(6),CIB(6)
COMMON TCI,TCO,PL,PA,PO,COX,CIX,COB,CIB,XL,XN,BE,SB,CB,SA,CA,CLN
COMMON F,G,H,BK,GA,RT,TO,ST,CT,BR,BT
S1=SIN(ANG)
C1=COS(ANG)
C2=C1*C1
C3=C1*C2
C5=C3*C2
C7=C5*C2
C9=C7*C2
C11=C9*C2
C13=C11*C2
C15=C13*C2
C17=C15*C2
C19=C17*C2
C21=C19*C2
S2=S1*S1
S3=S2*S1
S5=S3*S2
S7=S5*S2
S9=S7*S2
S11=S9*S2
B1=C1/S1
B3=C1/S3
B5=C1/S5
B7=C1/S7
B9=C1/S9
B11=C1/S11
TCI(1)=2.*C1
TCI(2)=-3.*C1*S2*S2
TCI(3)=.25*(35.*C9-120.*C7+150.*C5-80.*C3+15.*C1)
TCI(4)=.125*(-35.*C1+350.*C3-1281.*C5+2324.*C7-2261.*C9
1+1134.*C11-231.*C13)
TCI(5)=1./64.*(315.*C1-5040.*C3+29484.*C5-89280.*C7+158490.*C9
1-172080.*C11+112860.*C13-41184.*C15+6435.*C17)
TCI(6)=1./128.*(-693.*C1+16170.*C3-136521.*C5+605880.*C7-1632730.
1*C9+2855292.*C11-3326730.*C13+2572856.*C15-1271985.*C17+364650.*
2C19-46189.*C21)
TCO(1)=2.*B1
TCO(2)=4.*B3-7.*B1
TCO(3)=6.*B5-27.*B3+24.75*B1
TCO(4)=8.*B7-66.*B5+143.*B3-715./8.*B1
TCO(5)=10.*B9-130.*B7+487.5*B5-5525./8.*B3+20995./64.*B1
TCO(6)=12.*B11-225.*B9+1275.*B7-24225./8.*B5+101745./32.*B3
1-156009./128.*B1
RETURN
END

```

```

SUBROUTINE LPOL(AGI)
DIMENSION PL(11),PA(11),PO(11),COX(200,6),CIX(200,6),TCI(6),TCO(6)
DIMENSION COB(6),CIB(6)
COMMON TCI,TCO,PL,PA,PO,COX,CIX,COB,CIB,XL,XN,BE,SB,CB,SA,CA,CLN
COMMON F,G,H,BK,GA,RT,TO,ST,CT,BR,BT
S1=SIN(AGI)
C1=COS(AGI)
C2=C1*C1
C3=C2*C1
C4=C2*C2
C5=C4*C1
C6=C3*C3
C7=C3*C4
C8=C4*C4
C9=C4*C5
C10=C5*C5
PL(1)=S1
PL(2)=3.*S1*C1
PL(3)=1.5*S1*(5.*C2-1.)
PL(4)=2.5*S1*(7.*C3-3.*C1)
PL(5)=S1/8.*(315.*C4-210.*C2+15.)
PL(6)=S1/16.*(1386.*C5-1260.*C3+210.*C1)
PL(7)=S1/16.*(3003.*C6-3465.*C4+945.*C2-35.)
PL(8)=S1/128.*(-2520.*C1+27720.*C3-72072.*C5+51480.*C7)
PL(9)=S1/128.*(315.-13860.*C2+90090.*C4-180180.*C6+109395.*C8)
PL(10)=S1/256.*(6930.*C1-120120.*C3+540540.*C5-875160.*C7+461890.
1*C9)
PL(11)=S1/256.*(-693.+45045.*C2-450450.*C4+1531530.*C6-2078505.*C8
1+969969.*C10)
RETURN
END

```

```

SUBROUTINE FPH(XX)
DIMENSION PL(11),PA(11),PO(11),COX(200,6),CIX(200,6),TCI(6),TCO(6)
DIMENSION COB(6),CIB(6)
COMMON TCI,TCO,PL,PA,PO,COX,CIX,COB,CIB,XL,XN,BE,SB,CB,SA,CA,CLN
COMMON F,G,H,BK,GA,RT,TO,ST,CT,BR,BT
1 IF (XL/SB-XX) 2,2,4
2 SP=0
  X=XL/XX
  M=0
  DO 3 I=1,6
    K=I+M
    Z=FLOAT(K)
    W=Z+1.
    SP=SP+PO(I)/W*(COB(I)*X**W)
3 M=M+1
  F=1.-CLN*SP
  GO TO 6
4 V=XL/XX
  SP=0
  SA=V
  ALF=ASIN(V)
  CA=COS(ALF)
  CALL COMC(ALF)
  CALL LPOL(ALF)
  X=XX/XL
  M=0
  DO 5 I=1,6
    K=I+M
    Z=FLOAT(K)
    W=Z+1.
    SP1=X**Z*XX*PL(K)*2.*SA**W/(XL*CA)-V**Z*XL*2.*PL(K)/(XL*CA*SA**Z)
    SP1=1./(Z*W)*SP1
    SP=SP+PO(I)*(1./Z*X**Z*(CIB(I)-TCI(I))-1./W*V**W*TCO(I)-SP1 )
5 M=M+1
  F=1.+CLN*SP
6 RETURN
END

```

```

SUBROUTINE GAM(XX)
DIMENSION PL(11),PA(11),PO(11),COX(200,6),CIX(200,6),TCI(6),TCO(6)
DIMENSION COB(6),CIB(6)
COMMON TCI,TCO,PL,PA,PO,COX,CIX,COB,CIB,XL,XN,BE,SB,CB,SA,CA,CLN
COMMON F,G,H,BK,GA,RT,TO,ST,CT,BR,BT
IF (XL/SB-XX) 2,2,4
2 SP=0
X=XL/XX
M=0
DO 3 I=1,6
K=I+M
Z=FLOAT(K)
SP=SP+COB(I)/Z*PO(I)*X**K
3 M=M+1
G=-1./(2.*XN)*SP
GO TO 6
4 V=XL/XX
SP=0
ALF=ASIN(V)
SA=V
CA=COS(ALF)
X=XX/XL
M=0
DO 5 I=1,6
K=I+M
Z=FLOAT(K)
W=Z+1.
SP1=2.*V**(K-1)*PL(K)/(CA*SA**K)
SP1=SP1-2.*X**(K+2)*(SA**(K+1))/CA*PL(K)-W*V**Z*TCO(I)
SP=SP+PO(I)/(Z*W)*(Z*X**Z*(CIB(I)-TCI(I))+SP1)
5 M=M+1
G= 1./(2.*XN)*SP
6 RETURN
END

```

```

SUBROUTINE QUE(R,J)
DIMENSION PL(11),PA(11),PO(11),COX(200,6),CIX(200,6),TCI(6),TCO(6)
DIMENSION COB(6),CIB(6)
COMMON TCI,TCO,PL,PA,PO,COX,CIX,COB,CIB,XL,XN,BE,SB,CB,SA,CA,CLN
COMMON F,G,H,BK,GA,RT,TO,ST,CT,BR,BT
ST=SIN(TO)
CT=COS(TO)
CALL LPOL(TO)
SP=0.
RP=0
TP=0
QP=0
SL=XL/SB
IF (R=XL) 3,3,2
2 IF (SL=R) 7,7,5
3 X=R/XL
M=0
DO 4 I=1,6
K=M+I
Z=FLOAT(K)
W=Z+1.
SP=SP+PL(K)/(Z*W)*X**K*CIB(I)
IF (K .GT. 1) QP=PL(K-1)/ST
RP=RP+1./Z*X**(K-1)*CIB(I)*(CT/ST*PL(K)-QP)
TP=TP+CIB(I)/K*X**(K-1)*PL(K)
4 M=M+1
BR=BK*RP
BT=-BK*TP
H=2.*GA/(R*ST)+CLN*SP
GO TO 9
5 X=R/XL
V=XL/R
ALP=ASIN(XL/R)
SA=SIN(ALP)
CA=COS(ALP)
CALL LPOL(ALP)
DO 1 I=1,11
1 PA(I)=PL(I)
CALL LPOL(TO)
M=0
DO 6 I=1,6
K=I+M
Z=FLOAT(K)
W=Z+1.
IF (K .GT. 1) QP=PL(K-1)/ST

```

```

SP=SP+PL(K)/(Z*W)*(X**K*(CIB(I)-CIX(J,I))+V**W*COX(J,I))
RP=RP+1./Z*(X**(K-1)*(CIB(I)-CIX(J,I))+V**(K+2)*COX(J,I))
1*(CT*PL(K)/ST-QP)
TP1=2.*V**W*PA(K)/(CA*SA**K)-2.*SA**W/CA*PA(K)*X**K
TP1=TP1-K*COX(J,I)*V**(K+2)+W*X**(K-1)*(CIB(I)-CIX(J,I))
TP=TP+PL(K)/(Z*W)*TP1
6 M=M+1
BR=BK*RP
BT=-BK*TP
H=2.*GA/(R*ST)+CLN*SP
GO TO 9
7 X=XL/R
M=0
DO 8 I=1,6
K=M+I
Z=FLOAT(K)
W=Z+1.
IF (K .GT. 1) QP=PL(K-1)/ST
TP=TP+PL(K)/W*COB(I)*X**(K+2)
RP=RP+COB(I)/W*X**(K+2)*(PL(I)*CT/ST-QP)
SP=SP+PL(K)/(Z*W)*X**W*COB(I)
8 M=M+1
BR=BK*RP
BT= BK*TP
H=2.*GA/(R*ST)+CLN*SP
9 RETURN
END

```

```
FUNCTION FX(Q,RT2,R)
  IF (ABS(Q)-1.) 1,3,3
1  IF (R-RT2) 4,6,6
4  FX=.5*(1.-Q)
   GO TO 8
6  FX=1.
   GO TO 8
3  IF (Q) 6,10,10
10 FX=0.
8  RETURN
END
```

DOCUMENT CONTROL DATA - R&D

(Security classification of title, body of abstract and indexing annotation must be entered when the overall report is classified)

1. ORIGINATING ACTIVITY <i>(Corporate author)</i> Research Laboratories Brown Engineering Company, Inc. Huntsville, Alabama		2a. REPORT SECURITY CLASSIFICATION Unclassified	
		2b. GROUP N/A	
3. REPORT TITLE "Space Radiation Shielding with the Magnetic Field of a Cylindrical Solenoid"			
4. DESCRIPTIVE NOTES <i>(Type of report and inclusive dates)</i> Technical Note, June 1966			
5. AUTHOR(S) <i>(Last name, first name, initial)</i> McDonald, P. F. ; Buntyn, T. J.			
6. REPORT DATE June 1966	7a. TOTAL NO. OF PAGES 67	7b. NO. OF REFS 23	
8a. CONTRACT OR GRANT NO. NAS8-20166	9a. ORIGINATOR'S REPORT NUMBER(S) TN R-203		
b. PROJECT NO. N/A	9b. OTHER REPORT NO(S) <i>(Any other numbers that may be assigned this report)</i> None		
c.			
d.			
10. AVAILABILITY/LIMITATION NOTICES None			
11. SUPPLEMENTARY NOTES None		12. SPONSORING MILITARY ACTIVITY Research Projects Laboratory George C. Marshall Space Flight Center NASA	
13. ABSTRACT The charged-particle radiation shielding characteristics of magnetic fields generated by right circular solenoids are analyzed using Störmer's theory. Allowed and forbidden regions for unbound particle motion are obtained and shielded volumes are presented in parametric form. The results are applicable over a wide range of particle energies and solenoid parameters through the Störmer transformation.		14. KEY WORDS magnetic shielding radiation shielding Störmer's theory charged particle motion space radiation cylindrical solenoid shielded volume Liouville's theorem	